Authors: Yukihisa Goto[1, 2, 3, *], Yasuhiro Kadota[1, *], Malick Mbengue[4, 5], Jennifer D Lewis[6, 7, 8], Hidenori Matsui[9, 10], Noriko Maki[1], Jan Sklenar[4], Paul Derbyshire[4], Arisa Shibata[1], Yasunori Ichihashi[1, 11], David S. Guttman[6], Hirofumi Nakagami[9, 12], Takamasa Suzuki[13], Frank L.H. Menke[4], Silke Robatzek[4, 14], Darrell Desveaux[6], Cyril Zipfel[3, 4], Ken Shirasu[1, 2]

Affiliations:

[1] RIKEN Center for Sustainable Resource Science (CSRS), Plant Immunity Research Group, Suehiro-cho 1-7-22 Tsurumi-ku, Yokohama, Kanagawa, 230-0045, Japan

[2] Graduate school of Science, The University of Tokyo, 7-3-1, Hongo, Bunkyo-ku, Tokyo, 113-8654, Japan

[3] Institute of Plant and Microbial Biology, Zurich-Basel Plant Science Center, University of Zurich, Zollikerstrasse 107, CH-8008 Zurich, Switzerland

[4] The Sainsbury Laboratory, University of East Anglia, Norwich Research Park, Norwich NR4 7UH, United Kingdom

[5] Laboratoire de Recherche en Sciences Végétales, Université de Toulouse, CNRS, UPS, Toulouse INP, France.

[6] Department of Cell and System Biology and Centre for the Analysis of Genome Function and Evolution, University of Toronto, 25 Willcocks Street, Toronto, ON M5S 3B2, Canada

[7] Plant Gene Expression, United States Department of Agriculture, Agricultural Research Service, Albany, CA

[8] Department of Plant and Microbial Biology, University of California Berkeley,

Berkeley, California, USA.

[9] RIKEN CSRS, Plant Proteomics Research Unit, Suehiro-cho 1-7-22 Tsurumi-ku, Yokohama 230-0045, Japan

[10] Graduate School of Environmental and Life Science, Okayama University, Okayama, Japan.

[11] RIKEN BioResource Research Center, Tsukuba, Ibaraki 305-0074, Japan

[12] Protein Mass Spectrometry, Max Planck Institute for Plant Breeding Research, 50829 Cologne, Germany.

[13] College of Bioscience and Biotechnology, Chubu University, Kasugai, 487-0027, Japan.

[14] LMU Biocentre, Ludwig-Maximilian-University of Munich, Grosshaderner Strasse 4, 82152 Martinsried, Germany

* These authors contributed equally to this work.

Corresponding authors:

Yasuhiro Kadota, yasuhiro.kadota@riken.jp

Ken Shirasu, ken.shirasu@riken.jp

Title: The leucine-rich repeat receptor kinase QSK1 is a novel regulator of PRR-RBOHD complex and is employed by the bacterial effector HopF2$_{Pto}$ to modulate plant immunity

Short title: HopF2$_{Pto}$ interacts with QSK1 to suppress immunity

One Sentence Summary: QSK1, a novel component in the plant immune receptor complex, downregulates these receptors and phytocytokines, and is exploited by bacterial effector HopF2$_{Pto}$ to desensitize plants to pathogen attack.

The author(s) responsible for distribution of materials integral to the findings presented in this article in accordance with the policy described in the Instructions for Authors (https://academic.oup.com/plcell/pages/General-Instructions) are: Yasuhiro Kadota, yasuhiro.kadota@riken.jp and Ken Shirasu, ken.shirasu@riken.jp.

Abstract

Plants detect pathogens using cell-surface pattern recognition receptors (PRRs) like EFR and FLS2, which recognize bacterial EF-Tu and flagellin, respectively. These PRRs, belonging to the leucine-rich repeat receptor kinase (LRR-RK) family, activate the production of reactive oxygen species via the NADPH oxidase RBOHD. The PRR-RBOHD complex is tightly regulated to prevent unwarranted or exaggerated immune responses. However, certain pathogenic effectors can subvert these regulatory mechanisms, thereby suppressing plant immunity. To elucidate the intricate dynamics of the PRR-RBOHD complex, we conducted a comparative co-immunoprecipitation analysis using EFR, FLS2, and RBOHD. We identified QSK1, an LRR-RK, as a novel component of the PRR-RBOHD complex. QSK1 functions as a negative regulator of PRR-triggered immunity (PTI) by downregulating the abundance of FLS2 and EFR. QSK1 is targeted by the bacterial effector HopF2$_{Pto}$, a mono-ADP ribosyltransferase, resulting in the reduction of FLS2 and EFR levels through both transcriptional and transcription-independent pathways, thereby inhibiting PTI. Furthermore, HopF2$_{Pto}$ reduces transcript levels of *PROSCOOP* genes encoding important stress-regulated phytocytokines and their receptor MIK2. Importantly, HopF2$_{Pto}$ requires QSK1 for its accumulation and virulence functions within plants. In summary, our results provide novel insights into the mechanism by which HopF2$_{Pto}$ employs QSK1 to desensitize plants to pathogen attack.

Introduction

Plants and pathogens are in a perpetual evolutionary arms race. A fundamental aspect of the plant's defense mechanism lies in its capability to detect microbial molecules, particularly pathogen-associated molecular patterns (PAMPs) as well as endogenous danger molecules that are released from damaged or dying cells, known as damage-associated molecular patterns (DAMPs). These PAMPs and DAMPs are recognized by specialized cell-surface receptors known as pattern recognition receptors (PRRs) (Macho and Zipfel, 2014). Among those, leucine-rich repeat receptor-kinases (LRR-RKs) play a central role in the recognition of PAMPs and DAMPs. For instance, ELONGATION Factor-TU (EF-Tu) RECEPTOR (EFR) and FLAGELLIN SENSING2 (FLS2) detect bacterial EF-Tu and flagellin, respectively. The binding of flg22 or elf18 (the immunogenic peptides of flagellin or EF-Tu, respectively) to FLS2 and EFR induces their instant association with the coreceptor LRR-RK BRI1-ASSOCIATED RECEPTOR KINASE 1 (BAK1) and concomitant phosphorylation of both proteins to initiate PRR-triggered immunity (PTI) (Chinchilla et al., 2007; Heese et al., 2007; Roux et al., 2011). Subsequently, the PRR-BAK1 complex activates receptor-like cytoplasmic kinases (RLCKs) such as BOTRYTIS INDUCED KINASE 1 (BIK1) by phosphorylation (Lu et al., 2010; Zhang et al., 2010; Liu et al., 2013). PRRs further form a complex with the NADPH oxidase RESPIRATORY BURST OXIDASE HOMOLOG D (RBOHD), which is phosphorylated by activated BIK1, resulting in the rapid generation of reactive oxygen species (ROS) (Kadota et al., 2014; Li et al., 2014; Kadota et al., 2015). In addition, phosphorylated BIK1 activates Ca^{2+} channels, including

106 OSCA1.3 (HYPEROSMOLALITY-GATED Ca^{2+}-PERMEABLE CHANNEL1.3),
107 CNGC2 (CYCLIC NUCLEOTIDE-GATED CHANNEL2), and CNGC4,
108 particularly under specific Ca^{2+} concentrations (Tian et al., 2019; Thor et al.,
109 2020). This activation leads to an increase in cytoplasmic Ca^{2+} concentration,
110 subsequently stimulating Ca^{2+}-dependent protein kinases (Boudsocq et al.,
111 2010). Furthermore, BIK1 phosphorylates the non-canonical Gα protein, XLG2,
112 facilitating its translocation to the nucleus. This phenomenon inhibits MUT9-like
113 kinases, thereby removing the negative regulation of PTI (Liang et al., 2016; Ma
114 et al., 2022). The remarkable orchestration of signal transduction within PRR
115 complexes allows plants to mount swift and effective immune responses at
116 the very site of infection.

117 To overcome effective plant immunity, the pathogens deploy virulence
118 effectors to target and dampen immune signaling components (Dou and Zhou,
119 2012). Effectors with high immunomodulatory activities, especially those that
120 suppress early PTI responses such as ROS production, MAPK activation, and
121 Ca^{2+} influx, often target PRRs or their associated components. For example,
122 AvrPto, a type III effector from *P. syringae*, directly inhibits the kinase activity of
123 FLS2 and EFR (Xiang et al., 2008). AvrPtoB functions as an E3 ligase,
124 catalyzing the polyubiquitination and degradation of FLS2, BAK1, and CERK1
125 (Goehre et al., 2008; Gimenez-Ibanez et al., 2009; Cheng et al., 2011). HopB1
126 associates with FLS2 and serves as a protease, cleaving activated BAK1 (Li et
127 al., 2016). The *Xanthomonas campestris* effector AvrAC employs a unique
128 uridylyl-transferase activity to impede the activation of BIK1 (Feng et al., 2012).
129 These findings highlight the utility of effectors that suppress early PTI responses

as valuable tools for identifying and confirming PRR complex components. Indeed, key regulators in the PRR complex, such as BIK1, and PBLs, were originally identified as targets of the bacterial effector AvrPphB, which possesses cysteine protease activity (Zhang et al., 2010). A comprehensive investigation of PRR complex components in conjunction with virulence effectors will shed light on the essential regulatory mechanisms governing PRR complexes and uncover how pathogens manipulate the PRR complex to enhance their virulence.

In this study, we used comparative immunoprecipitation (IP) analysis of EFR, FLS2, and RBOHD followed by mass-spectrometry (IP-MS) to identify components of mature PRR-RBOHD complexes situated at the plasma membrane. This investigation led to the identification of QIAN SHOU KINASE1 (QSK1), an LRR-RK, as a new component of this complex. Intriguingly, QSK1 plays a negative regulatory role in PTI, possibly by controlling the steady-state levels of PRRs. Our interaction assays further revealed an association between the bacterial effector HopF2$_{Pto}$ and QSK1. HopF2$_{Pto}$, a mono-ADP ribosyltransferase, reduces PRR protein levels through both transcriptional and transcription-independent mechanisms. Moreover, HopF2$_{Pto}$ disrupts the signaling induced by SERINE RICH ENDOGENOUS PEPTIDE (SCOOP) phytocytokines. Importantly, the accumulation and virulence activities of HopF2$_{Pto}$ within plants rely on QSK1. In summary, our findings provide insights into the mechanisms by which QSK1 modulates PRR abundance and how HopF2$_{Pto}$ exploits QSK1 to render plant cells insensitive to PAMPs, DAMPs and SCOOP phytocytokines.

154

Results

Identification of QSK1, a novel component of PRR-RBOHD complexes

To isolate components specific to mature PRR-RBOHD complexes at the plasma membrane, we employed a comparative IP-MS strategy with EFR, FLS2, and RBOHD. Given the distinct protein structures of PRRs and RBOHD, it is likely that associated regulatory proteins involved in protein modification, maturation, transport, and degradation processes differ. Therefore, proteins that can associate with EFR, FLS2, and RBOHD are the most likely candidates to be associated with mature PRR-RBOHD complexes. To mitigate potential false positives resulting from sticky proteins, we implemented two different IP systems: magnetic and agarose beads. Through IP of FLS2-GFP from the Arabidopsis *pFLS2:FLS2-GFP* line using anti-GFP magnetic beads, we identified 118 FLS2-associated candidates (Supplemental Data Set S1_1). We had previously performed an IP of EFR-GFP using anti-GFP magnetic beads from the *efr-1/pEFR:EFR-GFP* line, identifying 42 candidate EFR-associated proteins (Supplemental Data Set S1_2) (Kadota et al., 2014). Moreover, we previously identified 451 candidate RBOHD-associated proteins through IP of 3xFLAG-RBOHD from the *rbohD*/*pRBOHD:3xFLAG-RBOHD* line by using Anti-FLAG agarose and eluted 3xFLAG-RBOHD with free 3xFLAG peptides (Supplemental Data Set S1_3) (Goto et al., 2023). Venn diagram analysis of these candidates pinpointed thirteen proteins commonly associated with FLS2, EFR, and RBOHD (Fig. 1), including known components of PRR complexes such as BAK1 (Chinchilla et al., 2007; Heese et al., 2007; Roux et al., 2011), IMPAIRED OOMYCETE SUSCEPTIBILITY 1 (IOS1) (Yeh et al., 2016),

AUTOINHIBITED Ca^{2+}-ATPASE 10 (ACA10) (Frei dit Frey et al., 2012), and RBOHD (Kadota et al., 2014; Li et al., 2014). Additionally, several proteins are known to accumulate in detergent-resistant membrane compartments in response to flg22, including QSK1, ACA10, SYNTAXIN OF PLANTS 71 (SYP71), HYPERSENSITIVE INDUCED REACTION1 (HIR1), HIR4, and REMORIN 1.2 (REM1.2) (Keinath et al., 2010). These results validate the effectiveness of our comparative IP-MS approach for identifying members of mature PRR-RBOHD complexes.

QSK1 (AT3G02880) is of particular significance as multiple tryptic peptides could be identified in the IPs with FLS2, EFR, and RBOHD (Supplemental Data Set S2). Notably, transient expression of *QSK1-3xHA* in *Nicotiana benthamiana* led to significant reduction in flg22-induced ROS production (Goto et al., 2023) (Supplemental Fig. S1). QSK1 is an LRR-RK with five LRRs in its ectodomain (Isner et al., 2018; Wu et al., 2019). To independently validate the interaction of QSK1 with FLS2, EFR, and RBOHD in Arabidopsis, we generated α-QSK1 antibodies. IP of FLS2-GFP from the *pFLS2:FLS2-GFP* stable transgenic line revealed a clear ligand-independent association between FLS2-GFP and endogenous QSK1 (Fig. 2A), in contrast to the ligand-dependent FLS2-BAK1 interaction. Further, we conducted IP experiments with EFR-GFP and 3xFLAG-RBOHD from *efr-1/pEFR:EFR-GFP* and *rbohD/pRBOHD:3xFLAG-RBOHD*, respectively (Fig. 2, B to C). The data reveal that RBOHD and EFR form ligand-independent interactions with QSK1, suggesting that QSK1 is an integral component of the PRR-RBOHD complex prior to elicitation, and this association remains stable even after PAMP

203 treatment.

204 **QSK1 negatively regulates PTI.**

205 To elucidate the role of QSK1 in the regulation of PRR-RBOHD complexes, we
206 conducted comprehensive characterization of the Arabidopsis *qsk1* mutant
207 (SALK_ 019840) (Isner et al., 2018). The *qsk1* mutant harbors a T-DNA
208 insertion within the first exon, resulting in pronounced reduction in *QSK1*
209 transcript levels compared to Col-0 (Supplemental Fig. S2, A to B). In addition,
210 immunoblotting with α-QSK1 antibodies failed to detect the QSK1 protein in the
211 *qsk1* mutant (Supplemental Fig. S2C), indicating that *qsk1* is a null mutant. The
212 *qsk1* mutant exhibited a significant increase in ROS production in response to
213 flg22, elf18, and the DAMP peptide pep1 (Figs 3, A to B; Supplemental Fig.
214 S2D). Furthermore, this mutant also showed enhanced MAPK activation 15
215 minutes following flg22 treatment (Fig. 3C). Collectively, these results indicate
216 that QSK1 exerts a negative regulatory influence on PTI signaling pathways.

217 To gain further insights into the impact of QSK1 on disease resistance,
218 we assessed growth of the weakly virulent bacterial strain *Pto* DC3000 *COR*$^-$
219 which lacks the toxin coronatine (COR) responsible for inducing stomatal
220 reopening during infection (Melotto et al., 2006), and the non-adapted bacterium
221 *Pseudomonas syringae* pv. *Cilantro* (*Pci*) 0788-9, known to exhibit poor growth
222 on Col-0 plants (Lewis et al., 2008). Six-week-old Arabidopsis plants were
223 spray-inoculated with *Pto* DC3000 *COR*$^-$ and *Pci.* At three days post-inoculation
224 (dpi), *qsk1* demonstrated enhanced resistance compared to Col-0 (Fig. 3, D to
225 E). This highlights the significant role of QSK1 in the negative regulation of plant
226 resistance to bacterial disease.

To verify that the observed phenotype is due to the lack of *QSK1*, we generated the complementation line, *qsk1/pQSK1:QSK1-GFP*. This complementation reversed the enhanced PAMP-induced ROS production evident in the *qsk1* mutant (Supplemental Fig. S3, A to B). No morphological differences were observed among the *qsk1* mutant, *qsk1/pQSK1:QSK1-GFP* lines, and Col-0 (Supplemental Fig. S3C). These results confirm that the amplified PTI responses in the *qsk1* mutant are attributed to the absence of *QSK1*.

To further investigate the role of QSK1 in modulating PRR-RBOHD complexes, we generated two independent Arabidopsis transgenic lines overexpressing *QSK1-3×HA* under the control of the *CaMV 35S* promoter (*p35S:QSK1-3×HA*). These lines exhibited markedly elevated *QSK1* transcript levels compared to Col-0 (Supplemental Fig. S4A) and produced a significantly higher amount of QSK1-3xHA protein than the endogenous QSK1 (Supplemental Fig. S4B). Morphological evaluations highlighted that the *p35S:QSK1-3×HA* lines had a marginally reduced size compared to both Col-0 and the *qsk1* mutant (Supplemental Fig. S4C). In stark contrast to the *qsk1* mutant, the *p35S:QSK1-3×HA* lines exhibited notably diminished ROS production upon treatment with flg22 and elf18 in comparison to Col-0 (Fig. 4, A to B). Additionally, *p35S:QSK1-3×HA* lines displayed attenuated MAPK activation in response to flg22 (Fig. 4C) and showed reduced resistance to *Pto* DC3000 *COR*$^-$ and *Pci* compared to Col-0 (Fig. 4, D to E). These results confirm that *QSK1* plays an important role as a negative regulator in PTI in Arabidopsis.

To determine the subcellular localization of QSK1 in plant cells, we

transiently expressed a QSK1-GFP fusion protein in *N. benthamiana*. QSK1-GFP localizes at the plasma membrane (Supplemental Fig. S5, A to B). This subcellular localization was confirmed in Arabidopsis using a stable transgenic line, *qsk1*/*pQSK1:QSK1-GFP* (Supplemental Fig. S5C). Additionally, we examined the transcriptional response of *QSK1* to PAMPs. Treatment with flg22 and elf18 led to an increase in *QSK1* transcript levels, indicating its transcriptional upregulation upon PAMP recognition (Supplemental Fig. S6).

QSK1 negatively regulates PRR protein levels.

Since QSK1 negatively regulates both ROS production and MAPK activation, two distinct signaling events following PAMP recognition (Xu et al., 2014), we hypothesized that QSK1 might influence the activity or stability of PRRs. Immunoblotting showed elevated FLS2 protein abundance in the *qsk1* mutant relative to Col-0 and the complemented *qsk1*/*pQSK1:QSK1-GFP* lines, while BAK1 levels remained unaffected (Fig. 5A). Conversely, FLS2 protein levels were reduced in QSK1 overexpression lines (*p35S:QSK1-3×HA*) compared to Col-0 (Fig. 5B). This regulatory mechanism does not appear to operate at the transcriptional level since *FLS2* mRNA amounts were comparable among Col-0, *qsk1*, and *p35S:QSK1-3×HA lines* (Fig. 5C). Supporting this notion, *N. benthamiana* plants co-expressing *FLS2-GFP* and *QSK1-GFP* under the control of the p35S promoters exhibited reduced FLS2-GFP protein levels (Fig. 5D). Similarly, overexpression of *QSK1* led to a decline in EFR protein levels; the EFR-GFP levels in *pEFR:EFR-GFP/ p35S:QSK1-3×HA* line were lower than those in *pEFR:EFR-GFP* lines (Fig. 5E). Further investigation into the impact of

QSK1 on the subcellular distribution of FLS2-GFP, revealed that a notable reduction in plasma membrane localization when co-expressed with *QSK1* in the *pFLS2:FLS2-GFP*/*p35S:QSK1-3xHA* line (Fig. 5F). These results suggest that QSK1 exerts a negative regulatory effect on PRR protein accumulation at the plasma membrane.

To elucidate the mechanism behind QSK1's modulation of FLS2 protein levels, we employed a pharmacological approach, using an array of inhibitors: MG132 (proteasome x), Bafilomycin A1 (vacuolar-type- H^+-ATPase inhibitor), E-64d (cysteine protease inhibitor), TLCK (serine protease inhibitor), Wortmannin (phosphatidylinositol 3-kinase inhibitor), Brefeldin A (ER-Golgi transport inhibitor), Cycloheximide (protein synthesis inhibitor), and Concanamycin A (ConA, vacuolar-type- H^+-ATPase inhibitor) (Fig. 5G; Supplemental Fig. S7). Notably, ConA mitigated the QSK1-mediated reduction of both FLS2 and EFR levels (Fig. 5G). ConA is known to block vacuolar transport, thereby impeding autophagic degradation pathway as well as the endocytosis-mediated degradation pathway (Dettmer et al., 2006; Scheuring et al., 2011). These findings suggest that *QSK1* overexpression may facilitate vacuolar degradation of PRRs through the autophagy pathway or the endocytosis pathway.

HopF2$_{Pto}$-HA interacts with QSK1 and reduces FLS2 protein levels

QSK1 could represent a potential effector target as part of PRR complexes because plant pathogens often deploy virulence effectors to target the PRR complex to effectively suppress PTI. Our attention was drawn to HopF2$_{Pto}$ from *Pto* DC3000, renowned for its potent inhibition of early PTI responses (Wilton et

al., 2010; Wu et al., 2011; Hurley et al., 2014; Zhou et al., 2014), as a likely candidate effector targeting QSK1, for several reasons. Firstly, Khan et al., conducted enzyme-catalyzed proximity labeling of HopF2$_{Pto}$ (Proximity-dependent Biotin Identification (BioID)) (Khan et al., 2018) and identified QSK1 as one of the 19 biotinylated proteins. Secondly, we employed a combination of yeast two-hybrid methods with next-generation sequencing, known as QIS-seq (Lewis et al., 2012), and revealed QSK1 as one of the 15 potential targets (Fig. 6A; Supplemental Data Set S3_1). Thirdly, a comparative analysis of potential HopF2$_{Pto}$ interactors by QIS-seq (Quantitative Interactor Screening with Next-Generation Sequencing) and BioID, alongside PRR complex components, using a Venn diagram (Fig. 6A), highlighted QSK1 as the sole common factor across all three datasets (Fig. 6A; Supplemental Data Set S3_2). This finding aligns with previous IP-MS experiments by Hurley *et al*., which also listed QSK1 among the proteins interacting with HopF2$_{Pto}$ when expressed in Arabidopsis (Hurley et al., 2014).

To validate the interaction between HopF2$_{Pto}$-HA and endogenous QSK1 *in vivo*, we employed the dexamethasone (DEX)-inducible system in transgenic Arabidopsis carrying the *pDEX:HopF2$_{Pto}$-HA* construct. Our results show *in vivo* interaction between HopF2$_{Pto}$-HA and QSK1 upon DEX treatment (Fig. 6B). To assess the impact of HopF2$_{Pto}$ on PRR complexes, we examined the protein levels of FLS2, RBOHD, BAK1, and QSK1 with or without expression of *HopF2$_{Pto}$-HA* (Fig. 6C). Strikingly, HopF2$_{Pto}$-HA specifically diminished the protein levels of FLS2 without affecting the other proteins. The reduction in FLS2 coincided with an increase in the levels of HopF2$_{Pto}$-HA

following DEX treatment (Fig. 6D). Next, we examined the effects of HopF2$_{Pto}$-HA on the subcellular localization of FLS2-GFP (Fig. 6E). In the absence of HopF2$_{Pto}$-HA expression, FLS2-GFP predominantly localized to the plasma membrane. However, induction of *HopF2$_{Pto}$-HA* expression by DEX treatment led to a significant reduction of FLS2-GFP at the plasma membrane.

The catalytic residue D175 of HopF2$_{Pto}$ is required for its virulence function.

A mutation in the catalytic residue D175 (D175A) of HopF2$_{Pto}$ leads to a significant reduction of its virulence, indicating the indispensable role of mono-ADP ribosylation (MARylation) in the functionality of HopF2$_{Pto}$ (Wilton et al., 2010). Notably, DEX-induced expression of *HopF2$_{Pto}$(D175A)-HA* did not decrease FLS2 protein levels (Fig. 7A), suggesting that MARylation activity is essential for HopF2$_{Pto}$'s ability to deplete FLS2. To further investigate the effects of HopF2$_{Pto}$ and its MARylation activity on FLS2 during infection, we introduced both the wild-type HopF2$_{Pto}$-HA and its D175A mutant into the non-pathogenic bacteria *Pseudomonas fluorescens* Pf0-1 (Fig. 7B). We selected *P. fluorescens* Pf0-1 due to its absence of virulence effectors, allowing a focused examination of HopF2$_{Pto}$ effects. The *bak1-5 bkk1* double mutants were infected with these modified bacteria. Employing *bak1-5 bkk1* mutants aimed to minimize the PTI-induced FLS2 accumulation during infection, although the suppression of FLS2 accumulation after bacterial inoculation was not complete. Infection with *P. fluorescens* Pf0-1 harboring *HopF2$_{Pto}$-HA* for ten hours resulted in increased levels of HopF2$_{Pto}$-HA and a concurrent decrease in FLS2 levels,

compared to both untransformed *P. fluorescens* Pf0-1 and *P. fluorescens* Pf0-1 harboring *HopF2*$_{Pto}$(D175A)-*HA*. These data demonstrate that HopF2$_{Pto}$-HA actively reduces FLS2 protein levels during infection and that the MARylation activity of HopF2$_{Pto}$ is required for this function. A pharmacological assay that involved a range of inhibitors, including ConA, E-64d, 3-Methyladenine (3-MA, PI3K inhibitor), BAF, Wm, BFA, MG132, and TLCK, showed that none of these inhibitors succeeded in counteracting the FLS2 depletion induced by HopF2$_{Pto}$ (Supplemental Fig. S8).

HopF2$_{Pto}$ modulates the expression of immune-related genes in Arabidopsis.

To explore the influence of HopF2$_{Pto}$ on plant immune responses, RNA-seq analysis was performed on Arabidopsis Col-0 and *pDEX:HopF2*$_{Pto}$*-HA* seedlings, post 24-h treatment with either DMSO or DEX. The multidimensional scaling plot displayed consistent global gene expression patterns across all four biological replicates for both treatments (Supplemental Fig. S9A). Notably, the *pDEX:HopF2*$_{Pto}$*-HA* line exhibited significant transcriptional changes upon DEX treatment, whereas DEX treatment in Col-0 led to only minor alterations in gene expression compared to those in the Col-0 and *pDEX:HopF2*$_{Pto}$*-HA* lines treated with DMSO.

To differentiate gene expression changes induced by HopF2$_{Pto}$ from those solely caused by DEX, we compared the gene expression in the DEX-treated *pDEX:HopF2*$_{Pto}$*-HA* line with DEX-treated Col-0. In the DEX-treated *pDEX:HopF2*$_{Pto}$*-HA* line, we observed an upregulation of 1399 genes and a

371 downregulation of 2,708 genes by at least twofold, along with 330 genes
372 upregulated and 879 genes downregulated by at least fourfold (Supplemental
373 Data Set S4). Gene Ontology (GO) enrichment analyses conducted on highly
374 upregulated (330 genes, log2 fold change ≥ 2, FDR ≤ 0.05) and highly
375 downregulated (879 genes, log2 fold change ≤ -2, FDR ≤ 0.05) genes provided
376 insights into the biological significance of these transcriptional changes
377 (Supplemental Data Set S5_1 and S5_2). Remarkably, both upregulated and
378 downregulated genes were significantly associated with GO terms related to
379 biotic stress responses and immunity, underlining HopF2$_{Pto}$'s crucial role in
380 modulating specific immune-related genes in Arabidopsis.

381 To pinpoint genes distinctively affected by *HopF2$_{Pto}$* expression, self-
382 organizing map (SOM) clustering was applied to the most differentially
383 expressed genes, focusing on the top 25% based on their coefficient of
384 variation across samples. These genes were grouped into 12 clusters, reflecting
385 unique expression patterns in Col-0 and *pDEX:HopF2$_{Pto}$-HA* following either
386 DMSO or DEX treatment (Supplemental Fig. S9B; Supplemental Data Set S6).
387 Notably, genes in cluster 1 were exclusively upregulated by HopF2$_{Pto}$, whereas
388 those in cluster 2 were specifically downregulated. The GO enrichment analysis
389 revealed that both clusters were enriched in GO terms associated with biotic
390 stress responses and immunity (Supplemental Data Set S5_3 and S5_4), and
391 cluster 2 exhibited a pronounced enrichment for GO terms like “membrane”,
392 “cell periphery”, and “plasma membrane”. These observations suggest that
393 HopF2$_{Pto}$ selectively modulates gene expression related to immune response
394 and plasma membrane-associated proteins.

Given HopF2$_{Pto}$'s role in diminishing FLS2 levels, we assessed the transcript levels of known *PRRs* (Fig. 8A). Notably, our data showed that HopF2$_{Pto}$ significantly reduces the transcript levels of certain *PRRs*, such as *FLS2*, *LORE* (*LIPOOLIGOSACCHARIDE-SPECIFIC REDUCED ELICITATION,* a PRR for bacterial fatty acid metabolite 3-OH-C10:0)(Kutschera et al., 2019), and *MIK2* (*MALE DISCOVERER 1-INTERACTING RECEPTOR-LIKE KINASE 2*, a PRR for SCOOP phytocytokines) (Hou et al., 2021; Rhodes et al., 2021), as well as *IOS1*, an import regulator in PRR complexes (Yeh et al., 2016) (Supplemental Fig. S10). Such reduction in transcript levels likely contributes to HopF2$_{Pto}$'s suppression of PTI responses, as corroborated by our observation that HopF2$_{Pto}$ inhibits ROS production mediated by FLS2 and MIK2 (Supplemental Fig. S11).

HopF2$_{Pto}$ reduces transcript levels of most PROSCOOPs.

Beyond inhibiting *PRR* gene expression, HopF2$_{Pto}$ also downregulates the SCOOP phytocytokine signaling. SCOOP phytocytokines, exclusive to the Brassicaceae family, are a unique group of peptides that are cleaved from the C-terminus of their respective precursors, termed PROSCOOPs (Gully et al., 2019). Our transcriptomic analysis revealed that HopF2$_{Pto}$ significantly downregulates the transcript levels of multiple *PROSCOOPs*, especially *PROSCOOP7*, *8*, *10*, *12*, and *23* (Fig. 8B), while its effect on *PROPEPs* and *PROPIP1*, encoding other DAMP peptides is minimal. This suggests HopF2$_{Pto}$'s role in attenuating SCOOP phytocytokine signaling by downregulating both *PROSCOOPs* and *MIK2* gene expression.

HopF2$_{Pto}$ reduces EFR protein levels possibly through vacuolar degradation.

While HopF2$_{Pto}$ reduces the expression of *FLS2*, *LORE*, and *MIK2*, it does not affect the expression of other *PRRs* such as *EFR* and *PEPR1* (*PEP RECEPTOR1,* a PRR for Pep1 and Pep2 peptides) (Fig. 8A). Nevertheless, HopF2$_{Pto}$ effectively impairs ROS production and MAPK activation triggered by these PRRs (Supplemental Figs. S11 and S12), indicating that HopF2$_{Pto}$ may also employ a transcription-independent mechanism to inhibit PTI. This insight prompted further exploration into how HopF2$_{Pto}$ affects the EFR signaling pathway. We generated a homozygous *pDEX:HopF2$_{Pto}$-HA/pEFR:EFR-GFP* line to assess the impact of *HopF2$_{Pto}$-HA* expression on EFR-GFP levels. Remarkably, DEX-induced *HopF2$_{Pto}$-HA* expression led to a decrease in EFR protein levels, suggesting that HopF2$_{Pto}$ exerts its influence on EFR protein levels via transcription-independent mechanisms. Interestingly, ConA effectively countered the HopF2$_{Pto}$-mediated reduction in EFR protein levels (Fig. 9), implying that this reduction might occur via vacuolar degradation through either the autophagy pathway or the endocytosis pathway. Additionally, we assessed the effect of the proteasome inhibitor MG132, which only slightly inhibited the reduction in EFR protein levels.

HopF2$_{Pto}$ requires QSK1 for its stabilization.

To investigate the functional relationship between HopF2$_{Pto}$ and QSK1, we generated a *qsk1/ pDEX:HopF2$_{Pto}$-HA* homozygous line by crossing, and

checked the HopF2$_{Pto}$-mediated reduction of FLS2 protein in a *qsk1* knockout background (Fig. 10A). Remarkably, the absence of QSK1 significantly reduces HopF2$_{Pto}$'s ability to reduce FLS2 levels, showing the crucial role of QSK1 in HopF2$_{Pto}$ function. Intriguingly, HopF2$_{Pto}$-HA protein levels were decreased in the *qsk1* mutant, suggesting a potential dependence of HopF2$_{Pto}$-HA on QSK1 for both its accumulation and functionality in plants. Furthermore, RT-qPCR analysis showed comparable DEX-induced expression of *HopF2$_{Pto}$-HA* in both *pDEX:HopF2$_{Pto}$-HA* and *qsk1/ pDEX:HopF2$_{Pto}$-HA* lines (Fig.10B), suggesting that the dependency of HopF2$_{Pto}$ on QSK1 is likely at the protein level rather than transcriptionally.

To understand this functional relationship during infection, we introduced HopF2$_{Pto}$-HA into the *Pto* DC3000 strain and subsequently infected both Col-0 and *qsk1* mutants. At 24 h post-inoculation, HopF2$_{Pto}$-HA accumulated more in Col-0 than in the *qsk1* mutant (Fig. 10C), while FLS2 levels were lower in Col-0 relative to the *qsk1* mutant when infected with *Pto* DC3000 harboring *HopF2$_{Pto}$-HA*. Importantly, bacterial populations remained consistent between Col-0 and *qsk1* mutants at this time point (Supplemental Fig. S13). These findings strengthen our hypothesis that QSK1 is necessary for maintaining HopF2$_{Pto}$'s protein stability and its ability to diminish FLS2 protein during infection. The *qsk1* mutant was more resistant against *Pto* DC3000 *ΔhopF2 HopF2$_{Pto}$-HA* than Col-0 at 3 dpi, further supporting the importance of QSK1 in stabilizing and facilitating HopF2$_{Pto}$'s function during infection (Fig. 10D).

Discussion

In this study, we addressed the critical need for plants to precisely control the activity of PRR complexes, a safeguard against the detrimental outcomes of unexpected or excessive immune activation. We discovered QSK1 as a novel modulator of these complexes, primarily through its influence on the abundance of PRR proteins. Notably, our findings reveal an interaction between the type-III effector HopF2$_{Pto}$ and QSK1, which is pivotal for the stabilization of HopF2$_{Pto}$ within plants. Once stabilized by QSK1, HopF2$_{Pto}$ effectively inhibits SCOOP phytocytokine signaling and downregulates the cell's responses to PAMPs and DAMPs by reducing PRR protein levels (Supplemental Fig. S14).

QSK1 negatively regulates PTI through modulation of PRR protein levels.

A tomato homolog of QSK1, TOMATO ATYPICAL RECEPTOR-LIKE KINASE 1 (TARK1), acts as a negative regulator of immunity as shown by increased resistance to pathogens in *tark1*-knockout lines and enhances susceptibility in its overexpression lines (Guzman et al., 2020). This indicates a conserved role of QSK1 in PTI across species. In Arabidopsis, QSK1-like proteins, LRR1, RKL1, and RLK90 may similarly modulate PTI (Supplemental Fig. S15), supported by elevated ROS production in *lrr1* and *rkl1* mutants in response to flg22, elf18, and pep1, a phenotype shared with the *qsk1* mutant. These results suggest that these homologs may function redundantly with QSK1 in PTI.

QSK1, also known as ALK1 (Auxin-induced LRR Kinase1) and KIN7 (Kinase 7), influences channels and transporters through phosphorylation, such as activating the TPK1 potassium channel during stomatal closure (Isner et al.,

2018), and modifying the ABC transporter ABCG36, which affects export of the auxin precursor indole-3-butyric acid and the phytoalexin camalexin (Aryal et al., 2023). QSK1 is also involved in drought stress responses (Chen et al., 2021) and the regulation of callose-mediated plasmodesmata regulation and lateral root development during osmotic stress (Grison et al., 2019). Our study demonstrated an additional role for QSK1 in PTI regulation, by modulating PRR abundance, distinct from its known pathways. QSK1 was also shown to function as a co-receptor of Sucrose-induced Receptor Kinase 1 (SIRK1), facilitating the phosphorylation and activation of aquaporin PIP2;4 upon recognition of endogenous pep7 peptides (Wu et al., 2019; Wang et al., 2022). Our experiments showed no significant impact of this pathway on PTI responses (Supplemental Fig. S16), suggesting that FLS2 modulation by QSK1 does not depend on the pep7-SIRK1 signaling pathway.

We observed that *QSK1* overexpression leads to a reduction of FLS2 protein levels at the plasma membrane (Fig. 5). Additionally, ConA inhibits the QSK1-mediated reduction of both EFR and FLS2, implying that QSK1 induces the vacuolar degradation of the PRRs through autophagy or endocytosis (Fig. 5G). This aligns with recent findings showing that the LRR-RK ROOT MERISTEM GROWTH FACTOR 1 INSENSITIVE (RGI) recognizes the phytocytokine peptide GOLVEN2 (GLV2) and interacts with FLS2, enhancing its protein levels (Stegmann et al., 2022). Interestingly, the RGI3 ectodomain directly interacts with that of QSK1 and RLK902, and RGI4 ectodomain interacts with RKL1 *in vitro* (Smakowska-Luzan et al., 2018). The interaction between QSK1, RGIs, and their homologs might imply a complex interplay that

disrupts the GLV2-mediated interaction between RGI and FLS2. Such disruption could cause the degradation of GLV2-unbound FLS2. A comprehensive understanding of the intricate relationship between phytocytokine signaling and FLS2 homeostasis, especially QSK1's involvement remains a critical area for future research.

HopF2$_{Pto}$ decreases plant responsiveness to PAMPs, DAMPs and SCOOP phytocytokines by reducing PRR levels.

Previous studies have established HopF2$_{Pto}$ as a potent inhibitor of PTI responses such as ROS production, MAPK activation, and callose deposition (Wu et al., 2011; Hurley et al., 2014; Zhou et al., 2014). Our work shows an additional role for HopF2$_{Pto}$ in diminishing plant response to PAMPs, DAMPs, and SCOOP phytocytokines specifically through reducing PRR levels and *PROSCOOPs* transcript levels. Interestingly, HopU1, another effector encoding a MARylation enzyme from *Pto* DC3000 also modulates FLS2 protein levels, by targeting GRP7, an RNA-binding protein in FLS2 translation (Fu et al., 2007; Nicaise et al., 2013). Unlike HopU1, which does not affect steady-state FLS2 levels (Nicaise et al., 2013), HopF2$_{Pto}$ significantly reduces both baseline (Fig. 6, C to D) and post-infection FLS2 levels (Fig. 9B). Thus, *Pto* DC3000 employs these two distinct MARlyation enzyme-coding effectors to manipulate FLS2 regulation in various ways. Furthermore, the pathogen uses the ubiquitin ligase AvrPtoB to degrade FLS2 by polyubiquitinating its kinase domain (Goehre et al., 2008). These strategies collectively highlight the significance of PRR suppression in the virulence mechanism of pathogens like *Pto* DC3000.

538

539 **The Interplay of HopF2$_{Pto}$ with MIK2 and PRR expression in modulating**
540 **plant immunity responses**

541 HopF2$_{Pto}$ significantly reduces the transcript levels of important PRRs, including
542 FLS2, LORE, CARD1, RDA2, and MIK2, as well as a majority of *PROSCOOPs*.
543 Intriguingly, *mik2* mutants exhibit reduced flg22-triggered ROS production
544 (Rhodes et al., 2021), hinting at MIK2's role in maintaining baseline expression
545 of *FLS2* and *PROSCOOPs*, through subtle activation by SCOOP peptides. This
546 is further supported by the findings that MIK2 activation by SCOOP12 increases
547 *FLS2* and PROSCOOP transcripts (Hou et al., 2021). Therefore, HopF2$_{Pto}$'s
548 impact on FLS2 levels might involve disrupting this MIK2-dependent positive
549 feedback loop. However, the HopF2$_{Pto}$-induced reduction in FLS2 cannot be
550 solely attributed to MIK2 disruption. This is evident as HopF2$_{Pto}$ expression
551 completely inhibits flg22-induced responses, whereas *mik2* mutants still retain
552 some responsiveness to flg22 (Supplemental Figs. S11 and S12)(Rhodes et al.,
553 2021).

554

555 **Distinct mechanisms of PRR degradation by HopF2$_{Pto}$: Exploring**
556 **vacuolar degradation and transcript regulation**

557 ConA's inhibition of the *HopF2$_{Pto}$*-induced EFR reduction implies that
558 HopF2$_{Pto}$ might target EFR for vacuolar degradation. However, ConA does not
559 reverse HopF2$_{Pto}$'s reduction of FLS2 protein (Supplemental Fig. S8A),
560 possibly attributed to HopF2$_{Pto}$'s differential effects on their transcripts: steady-
561 state FLS2 transcripts are diminished, while EFR transcripts remain unaffected.

Consequently, even if ConA inhibits the vacuolar degradation of FLS2, the diminished levels of FLS2 transcripts may still limit its protein synthesis. In contrast, EFR protein loss under HopF2$_{Pto}$ might be mainly through vacuolar degradation. This distinction is highlighted by the more pronounced reduction of FLS2 and FLS2-mediated MAPKs activation than EFR by HopF2$_{Pto}$ (Figs. 6 and 9; Supplemental Fig. S12).

Previous studies have shown that signaling-inactive FLS2 undergoes degradation through selective autophagy with Orosomucoid (ORM) proteins as key autophagy receptors (Yang et al., 2019), while signaling-active FLS2 undergoes vacuolar degradation through endocytosis (Robatzek et al., 2006; Beck et al., 2012; Mbengue et al., 2016). HopF2$_{Pto}$ might exploit either pathway to diminish PRR protein levels. Despite our hypotheses, direct observation of EFR or FLS2 within autophagosomes or endosomes after expressing *HopF2$_{Pto}$* was not feasible, likely due to the low expression levels of *EFR-GFP* in our Arabidopsis transgenic lines (*pEFR:EFR-GFP*) and the reduced FLS2 transcript levels complicating detailed microscopic observation of FLS2-GFP in *pFLS2:FLS2-GFP* lines.

The MARylation activity of HopF2$_{Pto}$ is required for its virulence.

Our finding establishes the critical role of HopF2$_{Pto}$'s catalytic residue in MARylation for FLS2 protein reduction (Fig. 7). However, the exact mechanisms through which HopF2$_{Pto}$ influences transcriptome reprogramming changes and vacuolar degradation of PRRs via MARylation remain elusive. Previous studies demonstrated that HopF2$_{Pto}$ targets key regulators of the PTI signaling

586 pathway, including MKK5 and BAK1 (Wang et al., 2010; Zhou et al., 2014), as
587 well as RIN4 (Wilton *et al.*, 2010), impacting both PTI and ETI. It is plausible
588 that HopF2$_{Pto}$-mediated inhibition of MKK5 and BAK1 contributes to
589 transcriptome reprogramming, possibly by disrupting MIK2 activation by
590 SCOOP peptides (Hou et al., 2021; Rhodes et al., 2021). However, MKK5 and
591 BAK1 are unlikely candidates for HopF2$_{Pto}$-mediated autophagy and/or
592 endocytosis of PRRs, because both proteins are not part of a stable PRR
593 complex in the absence of PAMP treatment (Chinchilla et al., 2007). Instead,
594 HopF2$_{Pto}$ may MARylate other proteins to induce autophagy and/or endocytosis
595 of PRRs.

596 We propose several hypotheses for HopF2$_{Pto}$ induction of PRR
597 degradation. Firstly, HopF2$_{Pto}$ may MARylates and activates QSK1. This
598 activation could inhibit the RGI-FLS2 association, leading to PRR destabilization
599 and their subsequent degradation through autophagy and/or endocytosis. This
600 hypothesis is supported by the fact that both QSK1 and HopF2$_{Pto}$ induce
601 vacuolar degradation of PRRs (Figs 5, 6, and 9). Another hypothesis is that
602 HopF2$_{Pto}$ directly MARylates PRRs, altering their structural conformation to
603 enhance ORM protein binding and thus autophagy. In this scenario, QSK1
604 might serve as a scaffold, facilitating PRR MARylation. Lastly, HopF2$_{Pto}$ might
605 target G proteins, known to inhibit FLS2 autophagy (Miller et al., 2019). This is
606 supported by the fact that bacterial toxins predominantly MARylate Gα proteins
607 in animals (Ishiwata-Endo et al., 2020). Detecting HopF2$_{Pto}$'s MARylation *in*
608 *vivo* remains technically challenging, particularly direct observation of the
609 MARylation of QSK1 and PRRs. Future studies should focus on identifying

proteins MARylated by HopF2$_{Pto}$ *in vivo* and clarifying their roles in the vacuolar degradation of PRRs through autophagy and/or endocytosis.

HopF2$_{Pto}$ requires QSK1 for its stabilization and function

Our findings indicate that QSK1 plays a pivotal role in stabilizing HopF2$_{Pto}$ in plants, although its exact mechanism remains elusive. Notably, HopF2$_{Pto}$, known to possess a predicted myristoylation sequence essential for plasma membrane localization and virulence (Wilton et al., 2010), seems to stabilize when it interacts with QSK1, following myristoylation. This interaction may assist HopF2$_{Pto}$ in targeting the PRR complex. The complex interplay between QSK1 and HopF2$_{Pto}$, while not fully understood, indicates a broader role for QSK1 and its homologs in aiding virulence effectors across various plants. For instance, XopN, a virulence factor from *X. campestris*, interacts with TARK1, a tomato homolog of QSK1 (Kim et al., 2009; Guzman et al., 2020). In *tark1*-silenced plants, XopN's virulence function is notably reduced, suggesting that TARK1 is crucial for XopN functionality. Moreover, TARK1 may guide XopN to interact with tomato 14-3-3 isoform TFT1, a positive regulator of PTI in tomatoes (Taylor et al., 2012). This relationship mirrors that of HopF2$_{Pto}$-QSK1-PRR, though it remains unclear if TARK1 primarily maintains XopN protein stability, and facilitates its integration into the PRR complex.

631 **Methods**

632 **Plant materials and growth conditions**

633 *Arabidopsis thaliana* (L.) Heynh. Plants were grown on soil under an 8 h or 16 h
634 photoperiod at 23°C, or in a half-strength MS medium containing 1% sucrose
635 under a continuous light photoperiod at 23°C. *Nicotiana benthamiana* Domin.
636 Plants were soil-grown under a 16 h photoperiod at 25°C.

637

638 **Vector construction and generation**

639 To generate epiGreenB5-*p35S:QSK1-3×HA*, and epiGreenB5-*p35S:QSK1-*
640 *GFP*, CDS region of QSK1 was amplified by PCR with KoD FX neo (Toyobo,
641 Osaka, Japan) and the resulting PCR product was cloned into the epiGreenB5
642 (3*x*HA) and epiGreenB (eGFP) vectors between the *Cla*I and *Bam*HI restriction
643 sites with an In-Fusion HD Cloning Kit (Clontech, CA, USA) (Nekrasov et al.,
644 2009). To generate epiGreenB5-*pQSK1:QSK1-GFP,* an amplicon containing the
645 2000-bp promoter upstream of the start codon and the coding regions of QSK1
646 was cloned into the epiGreenB (eGFP) vectors between the *EcoRI* and *Bam*HI
647 restriction sites with In-Fusion HD Cloning Kit. pCAMBIA2300-*pFLS2:FLS2-*
648 *GFP* was described previously (Robatzek et al., 2006).

649

650 **Transgenic lines and T-DNA insertion lines**

651 Arabidopsis stable transgenic lines of *p35S:QSK1-3×HA* (epiGreenB5),
652 *p35S:QSK1-GFP* (epiGreenB5), and *qsk1/pQSK1:QSK1-GFP* (epiGreenB5)
653 were generated by the floral drop and floral dip methods. T-DNA insertion
654 mutant lines, *qsk1* (SALK_ 019840C), *lrr1* (WiscDsLoxHs082_03E), *rkl1*

(SALK_099094C), *sirk1* (SALK_125543C), and *pep7* (SALK_025824C) were obtained from the Arabidopsis Biological Resource Center at the Ohio State University. Previously published lines were: *bak1bkk1* (Roux et al., 2011), *fls2*, *pFLS2:FLS2-GFP* (Robatzek et al., 2006), *efr-1/pEFR:EFR-GFP*, *rbohD/pRBOHD:3xFLAG-gRBOHD* (Kadota et al., 2014), *pDEX:HopF2$_{Pto}$-HA* and its variant D175A (Wilton et al., 2010). Homozygous *pFLS2:FLS2-GFP/p35S:QSK1-3xHA, pEFR:EFR-GFP/p35S:QSK1-3xHA, qsk1*/*pDEX:HopF2$_{Pto}$*-HA, *pDEX:HopF2$_{Pto}$-HA*//*pFLS2:FLS2-GFP,* and *pDEX:HopF2$_{Pto}$*-HA//*pEFR:EFR-GFP* lines were generated by crossing homozygous lines and then selection by genotyping.

Generation of QSK1 antibody

A polyclonal anti-QSK1 antibody was produced by immunizing rabbits with a synthetic peptide (NH2-C+EEVSHSSGSPNPVSD-COOH) originating from the C-terminal region of QSK1 (Eurofins Scientific SE, Luxembourg).

Immunoblotting

Immunoblotting was performed with antibodies diluted in the blocking solution (5% nonfat milk in TBS with 0.1% [v/v] Tween) at the following dilutions: α-GFP antibody (ab290, Abcam, Cambridge, UK), 1:8,000; α-HA-horseradish peroxidase (HRP) (3F10, Roche, Basel, Switzerland), 1:5,000; α-FLAG-HRP (M2 monoclonal antibody, Sigma-Aldrich, St. Louis, MO, USA), 1:2000; α-FLS2 (Chinchilla et al., 2006), 1:1,000; α-BAK1 (Roux et al., 2011), 1:1000; α-QSK1,1:500, and α-rabbit-HRP conjugated antibody (NA934; GE Healthcare,

679 Chicago, IL, USA), 1:10,000. For detection of RBOHD, α-RBOHD (AS152962;
680 1:1,000; Agrisera, Vännäs, Sweden) antibody was diluted in Can Get Signal®
681 Solution 1 (Toyobo, Osaka, Japan) and the α-rabbit-HRP conjugated antibody
682 was diluted in Can Get Signal® Solution 2 to enhance the signal of
683 immunoblotting.
684
685 **Bacterial strains**
686 *Pto* DC3000 *ΔhopF2 HopF2*$_{Pto}$*-HA* was described previously (Wilton et al.,
687 2010). It is important to note that the native HopF2$_{Pto}$ has an ATA start codon,
688 which limits its expression. On the other hand, *Pto* DC3000 *ΔhopF2 HopF2*$_{Pto}$-
689 *HA* uses the more common ATG start codon, resulting in enhanced expression
690 of *HopF2*$_{pto}$*-HA* during the infection. To generate *Pseudomonas fluorescens*
691 (Pf0-1) *HopF2*$_{Pto}$*-HA* and *P. fluorescens* Pf0-1*HopF2*$_{Pto}$ (D175A)-*HA*, *P.*
692 *fluorescens* Pf0-1 was transformed with the expression vectors, *schF2/hopF2*$_{Pto}$
693 ^{ATG}*:HA* or *schF2/hopF2*$_{Pto}$^{ATG} (D175A)*:HA.*
694
695 **Statistical Analysis**
696 Statistical significances based on t-test and one-way ANOVA were determined
697 with GraphPad Prism6 software (GraphPad Software, San Diego, CA, USA).
698 Statistical data are provided in Supplemental Data Set S7.
699
700 **Other methods**
701 Chemical inhibitors were described in Methods S1. Protein extraction, IP**,**
702 protein identification by LC-MS/MS, ROS burst assay, MAPK activation assay,

703 bacterial infection assays, phylogenetic analyses, transient expression in *N.*
704 *benthamiana,* confocal microscopy analyses, RT-qPCR assay, QIS-Seq
705 analyses, RNA-seq and differential gene expression analyses, PCA with SOM
706 clustering, and GO term enrichment analyses were performed as described
707 previously (Lewis et al., 2012; Kadota et al., 2014; Goto et al., 2020; Goto et al.,
708 2023) with minor modifications detailed in Supplemental Methods S1. All
709 primers used in this study are listed in Supplemental Data Set S8.
710

711 **Acknowledgments**
712 We thank all members of the Shirasu lab for discussion. We thank Ayami
713 Furuta, Naomi Watanabe, Mamiko Kouzai, Mizuki Yamamoto, and Yoko Nagai
714 for their support of this project.
715

716 **Author contributions**
717 YK and MM performed IP experiments. JS, PD, and FLHM. performed LC-
718 MS/MS analyses. NM helped to generate plasmids. YK, YG, and HM
719 characterized the phenotype of the *qsk1* mutant and overexpression lines. JDL
720 performed QIS seq. YK and YG analyzed the effect of HopF2$_{Pto}$ on FLS2
721 homeostasis and the role of QSK1 for HopF2$_{Pto}$ function. AS, TS, YI performed
722 RNA-seq analyses and YK and YG analyzed the data. YK, DSG, HN, SR, DD,
723 CZ, and KS supervised the research. YK and YG wrote the draft manuscript. All
724 the authors commented on the manuscript.
725

726 **Funding**

727 The research was financially supported by JSPS KAKENHI Grant Numbers
728 16J00771 (to Y.G), 16H06186, 16KT0037, 20H02994, 21K19128 (to Y.K),
729 17H06172, 20H05909, 22H00364 (to K.S), USDA ARS 2030-21000-046-00D
730 and 2030-21000-050-00D (JDL), as well as the Gatsby Charitable Foundation
731 (to F.L.H.M, C.Z., and S.R.), the Natural Sciences and Engineering Research
732 Council of Canada (DD and DSG), and the European Research Council (project
733 'PHOSPHinnATE', grant agreement No. 309858 to C.Z. and project "STORM",
734 grant agreement No. 311310 to S.R.).

735

736 **Data availability**

737 The data underlying this article are available in the article and in its online
738 supplementary material.

739

References

Aryal, B., Xia, J., Hu, Z., Stumpe, M., Tsering, T., Liu, J., Huynh, J., Fukao, Y., Glockner, N., Huang, H.Y., Sancho-Andres, G., Pakula, K., Ziegler, J., Gorzolka, K., Zwiewka, M., Nodzynski, T., Harter, K., Sanchez-Rodriguez, C., Jasinski, M., Rosahl, S., and Geisler, M.M. (2023). An LRR receptor kinase controls ABC transporter substrate preferences during plant growth-defense decisions. Curr Biol **33,** 2008-2023 e2008.

Beck, M., Zhou, J., Faulkner, C., MacLean, D., and Robatzek, S. (2012). Spatio-temporal cellular dynamics of the Arabidopsis flagellin receptor reveal activation status-dependent endosomal sorting. Plant Cell **24,** 4205-4219.

Boudsocq, M., Willmann, M.R., McCormack, M., Lee, H., Shan, L.B., He, P., Bush, J., Cheng, S.H., and Sheen, J. (2010). Differential innate immune signalling via Ca2+ sensor protein kinases. Nature **464,** 418-U116.

Chen, X., Wang, T., Rehman, A.U., Wang, Y., Qi, J., Li, Z., Song, C., Wang, B., Yang, S., and Gong, Z. (2021). Arabidopsis U-box E3 ubiquitin ligase PUB11 negatively regulates drought tolerance by degrading the receptor-like protein kinases LRR1 and KIN7. J Integr Plant Biol **63,** 494-509.

Cheng, W., Munkvold, K.R., Gao, H.S., Mathieu, J., Schwizer, S., Wang, S., Yan, Y.B., Wang, J.J., Martin, G.B., and Chai, J.J. (2011). Structural Analysis of Pseudomonas syringae AvrPtoB Bound to Host BAK1 Reveals Two Similar Kinase-Interacting Domains in a Type III Effector. Cell Host & Microbe **10,** 616-626.

Chinchilla, D., Bauer, Z., Regenass, M., Boller, T., and Felix, G. (2006). The Arabidopsis receptor kinase FLS2 binds flg22 and determines the specificity of flagellin perception. Plant Cell **18,** 465-476.

Chinchilla, D., Zipfel, C., Robatzek, S., Kemmerling, B., Nurnberger, T., Jones, J.D., Felix, G., and Boller, T. (2007). A flagellin-induced complex of the receptor FLS2 and BAK1 initiates plant defence. Nature **448,** 497-500.

Dettmer, J., Hong-Hermesdorf, A., Stierhof, Y.D., and Schumacher, K. (2006). Vacuolar H+-ATPase activity is required for endocytic and secretory trafficking in Arabidopsis. Plant Cell **18,** 715-730.

Dou, D.L., and Zhou, J.M. (2012). Phytopathogen Effectors Subverting Host Immunity: Different Foes, Similar Battleground. Cell Host & Microbe **12,** 484-495.

Feng, F., Yang, F., Rong, W., Wu, X.G., Zhang, J., Chen, S., He, C.Z., and Zhou, J.M. (2012). A Xanthomonas uridine 5 '-monophosphate transferase inhibits plant immune kinases. Nature **485,** 114-U149.

Frei dit Frey, N., Mbengue, M., Kwaaitaal, M., Nitsch, L., Altenbach, D., Haweker, H., Lozano-Duran, R., Njo, M.F., Beeckman, T., Huettel, B., Borst, J.W., Panstruga, R.,

and Robatzek, S. (2012). Plasma membrane calcium ATPases are important components of receptor-mediated signaling in plant immune responses and development. Plant Physiology **159,** 798-+.

Fu, Z.Q., Guo, M., Jeong, B.R., Tian, F., Elthon, T.E., Cerny, R.L., Staiger, D., and Alfano, J.R. (2007). A type III effector ADP-ribosylates RNA-binding proteins and quells plant immunity. Nature **447,** 284-288.

Gimenez-Ibanez, S., Hann, D.R., Ntoukakls, V., Petutschnig, E., Lipka, V., and Rathjen, J.P. (2009). AvrPtoB Targets the LysM Receptor Kinase CERK1 to Promote Bacterial Virulence on Plants. Current Biology **19,** 423-429.

Goehre, V., Spallek, T., Haeweker, H., Mersmann, S., Mentzel, T., Boller, T., de Torres, M., Mansfield, J.W., and Robatzek, S. (2008). Plant Pattern-Recognition Receptor FLS2 Is Directed for Degradation by the Bacterial Ubiquitin Ligase AvrPtoB. Current Biology **18,** 1824-1832.

Goto, Y., Maki, N., Ichihashi, Y., Kitazawa, D., Igarashi, D., Kadota, Y., and Shirasu, K. (2020). Exogenous Treatment with Glutamate Induces Immune Responses in Arabidopsis. Mol Plant Microbe Interact **33,** 474-487.

Goto, Y., Maki, N., Sklenar, J., Derbyshire, P., Menke, F.L.H., Zipfel, C., Kadota, Y., and Shirasu, K. (2023). The phagocytosis oxidase/Bem1p domain-containing proteinPB1CP negatively regulates the NADPH oxidase RBOHD inplant immunity. New Phytologist, 2023 accepted.

Grison, M.S., Kirk, P., Brault, M.L., Wu, X.N., Schulze, W.X., Benitez-Alfonso, Y., Immel, F., and Bayer, E.M. (2019). Plasma Membrane-Associated Receptor-like Kinases Relocalize to Plasmodesmata in Response to Osmotic Stress. Plant Physiol **181,** 142-160.

Gully, K., Pelletier, S., Guillou, M.C., Ferrand, M., Aligon, S., Pokotylo, I., Perrin, A., Vergne, E., Fagard, M., Ruelland, E., Grappin, P., Bucher, E., Renou, J.P., and Aubourg, S. (2019). The SCOOP12 peptide regulates defense response and root elongation in Arabidopsis thaliana. J Exp Bot **70,** 1349-1365.

Guzman, A.R., Kim, J.G., Taylor, K.W., Lanver, D., and Mudgett, M.B. (2020). Tomato Atypical Receptor Kinase1 Is Involved in the Regulation of Preinvasion Defense. Plant Physiol **183,** 1306-1318.

Heese, A., Hann, D.R., Gimenez-Ibanez, S., Jones, A.M., He, K., Li, J., Schroeder, J.I., Peck, S.C., and Rathjen, J.P. (2007). The receptor-like kinase SERK3/BAK1 is a central regulator of innate immunity in plants. Proc Natl Acad Sci U S A **104,** 12217-12222.

Hou, S., Liu, D., Huang, S., Luo, D., Liu, Z., Xiang, Q., Wang, P., Mu, R., Han, Z., Chen, S., Chai, J., Shan, L., and He, P. (2021). The Arabidopsis MIK2 receptor elicits

immunity by sensing a conserved signature from phytocytokines and microbes. Nat Commun **12,** 5494.

Hurley, B., Lee, D., Mott, A., Wilton, M., Liu, J., Liu, Y.C., Angers, S., Coaker, G., Guttman, D.S., and Desveaux, D. (2014). The Pseudomonas syringae type III effector HopF2 suppresses Arabidopsis stomatal immunity. PLoS One **9,** e114921.

Ishiwata-Endo, H., Kato, J., Stevens, L.A., and Moss, J. (2020). ARH1 in Health and Disease. Cancers (Basel) **12**.

Isner, J.C., Begum, A., Nuehse, T., Hetherington, A.M., and Maathuis, F.J.M. (2018). KIN7 Kinase Regulates the Vacuolar TPK1 K(+) Channel during Stomatal Closure. Curr Biol **28,** 466-472 e464.

Kadota, Y., Shirasu, K., and Zipfel, C. (2015). Regulation of the NADPH Oxidase RBOHD During Plant Immunity. Plant Cell Physiol **56,** 1472-1480.

Kadota, Y., Sklenar, J., Derbyshire, P., Stransfeld, L., Asai, S., Ntoukakis, V., Jones, J.D., Shirasu, K., Menke, F., Jones, A., and Zipfel, C. (2014). Direct regulation of the NADPH oxidase RBOHD by the PRR-associated kinase BIK1 during plant immunity. Mol Cell **54,** 43-55.

Keinath, N.F., Kierszniowska, S., Lorek, J., Bourdais, G., Kessler, S.A., Shimosato-Asano, H., Grossniklaus, U., Schulze, W.X., Robatzek, S., and Panstruga, R. (2010). PAMP (Pathogen-associated Molecular Pattern)-induced Changes in Plasma Membrane Compartmentalization Reveal Novel Components of Plant Immunity. Journal of Biological Chemistry **285,** 39140-39149.

Khan, M., Youn, J.Y., Gingras, A.C., Subramaniam, R., and Desveaux, D. (2018). In planta proximity dependent biotin identification (BioID). Sci Rep **8,** 9212.

Kim, J.G., Li, X., Roden, J.A., Taylor, K.W., Aakre, C.D., Su, B., Lalonde, S., Kirik, A., Chen, Y., Baranage, G., McLane, H., Martin, G.B., and Mudgett, M.B. (2009). Xanthomonas T3S Effector XopN Suppresses PAMP-Triggered Immunity and Interacts with a Tomato Atypical Receptor-Like Kinase and TFT1. Plant Cell **21,** 1305-1323.

Kutschera, A., Dawid, C., Gisch, N., Schmid, C., Raasch, L., Gerster, T., Schaffer, M., Smakowska-Luzan, E., Belkhadir, Y., Vlot, A.C., Chandler, C.E., Schellenberger, R., Schwudke, D., Ernst, R.K., Dorey, S., Huckelhoven, R., Hofmann, T., and Ranf, S. (2019). Bacterial medium-chain 3-hydroxy fatty acid metabolites trigger immunity in Arabidopsis plants. Science **364,** 178-181.

Lewis, J.D., Abada, W., Ma, W., Guttman, D.S., and Desveaux, D. (2008). The HopZ family of Pseudomonas syringae type III effectors require myristoylation for virulence and avirulence functions in Arabidopsis thaliana. J Bacteriol **190,** 2880-2891.

Lewis, J.D., Wan, J., Ford, R., Gong, Y., Fung, P., Nahal, H., Wang, P.W., Desveaux, D., and Guttman, D.S. (2012). Quantitative Interactor Screening with next-generation Sequencing (QIS-Seq) identifies Arabidopsis thaliana MLO2 as a target of the Pseudomonas syringae type III effector HopZ2. BMC Genomics **13,** 8.

Li, L., Kim, P., Yu, L., Cai, G., Chen, S., Alfano, J.R., and Zhou, J.M. (2016). Activation-Dependent Destruction of a Co-receptor by a Pseudomonas syringae Effector Dampens Plant Immunity. Cell Host Microbe **20,** 504-514.

Li, L., Li, M., Yu, L.P., Zhou, Z.Y., Liang, X.X., Liu, Z.X., Cai, G.H., Gao, L.Y., Zhang, X.J., Wang, Y.C., Chen, S., and Zhou, J.M. (2014). The FLS2-Associated Kinase BIK1 Directly Phosphorylates the NADPH Oxidase RbohD to Control Plant Immunity. Cell Host & Microbe **15,** 329-338.

Liang, X.X., Ding, P.T., Liang, K.H., Wang, J.L., Ma, M.M., Li, L., Li, L., Li, M., Zhang, X.J., Chen, S., Zhang, Y.L., and Zhou, J.M. (2016). Arabidopsis heterotrimeric G proteins regulate immunity by directly coupling to the FLS2 receptor. Elife **5,** e13568.

Liu, Z.X., Wu, Y., Yang, F., Zhang, Y.Y., Chen, S., Xie, Q., Tian, X.J., and Zhou, J.M. (2013). BIK1 interacts with PEPRs to mediate ethylene-induced immunity. P Natl Acad Sci USA **110,** 6205-6210.

Lu, D.P., Wu, S.J., Gao, X.Q., Zhang, Y.L., Shan, L.B., and He, P. (2010). A receptor-like cytoplasmic kinase, BIK1, associates with a flagellin receptor complex to initiate plant innate immunity. P Natl Acad Sci USA **107,** 496-501.

Ma, M.M., Wang, W., Fei, Y., Cheng, H.Y., Song, B.B., Zhou, Z.Y., Zhao, Y., Zhang, X.J., Li, L., Chen, S., Wang, J.Z., Liang, X.X., and Zhou, J.M. (2022). A surface-receptor-coupled G protein regulates plant immunity through nuclear protein kinases. Cell Host & Microbe **30,** 1602-+.

Macho, A.P., and Zipfel, C. (2014). Plant PRRs and the activation of innate immune signaling. Mol Cell **54,** 263-272.

Mbengue, M., Bourdais, G., Gervasi, F., Beck, M., Zhou, J., Spallek, T., Bartels, S., Boller, T., Ueda, T., Kuhn, H., and Robatzek, S. (2016). Clathrin-dependent endocytosis is required for immunity mediated by pattern recognition receptor kinases. Proc Natl Acad Sci U S A **113,** 11034-11039.

Melotto, M., Underwood, W., Koczan, J., Nomura, K., and He, S.Y. (2006). Plant stomata function in innate immunity against bacterial invasion. Cell **126,** 969-980.

Miller, J.C., Lawrence, S.A., and Clay, N.K. (2019). Heterotrimeric G proteins promote FLS2 protein accumulation through inhibition of FLS2 autophagic degradation. bioRxiv, 438135.

Nekrasov, V., Li, J., Batoux, M., Roux, M., Chu, Z.H., Lacombe, S., Rougon, A., Bittel, P.,

Kiss-Papp, M., Chinchilla, D., van Esse, H.P., Jorda, L., Schwessinger, B., Nicaise, V., Thomma, B.P., Molina, A., Jones, J.D., and Zipfel, C. (2009). Control of the pattern-recognition receptor EFR by an ER protein complex in plant immunity. EMBO J **28,** 3428-3438.

Nicaise, V., Joe, A., Jeong, B.R., Korneli, C., Boutrot, F., Westedt, I., Staiger, D., Alfano, J.R., and Zipfel, C. (2013). Pseudomonas HopU1 modulates plant immune receptor levels by blocking the interaction of their mRNAs with GRP7. EMBO J **32,** 701-712.

Rhodes, J., Yang, H., Moussu, S., Boutrot, F., Santiago, J., and Zipfel, C. (2021). Perception of a divergent family of phytocytokines by the Arabidopsis receptor kinase MIK2. Nat Commun **12,** 705.

Robatzek, S., Chinchilla, D., and Boller, T. (2006). Ligand-induced endocytosis of the pattern recognition receptor FLS2 in Arabidopsis. Genes Dev **20,** 537-542.

Roux, M., Schwessinger, B., Albrecht, C., Chinchilla, D., Jones, A., Holton, N., Malinovsky, F.G., Tor, M., de Vries, S., and Zipfel, C. (2011). The Arabidopsis leucine-rich repeat receptor-like kinases BAK1/SERK3 and BKK1/SERK4 are required for innate immunity to hemibiotrophic and biotrophic pathogens. Plant Cell **23,** 2440-2455.

Scheuring, D., Viotti, C., Kruger, F., Kunzl, F., Sturm, S., Bubeck, J., Hillmer, S., Frigerio, L., Robinson, D.G., Pimpl, P., and Schumacher, K. (2011). Multivesicular bodies mature from the trans-Golgi network/early endosome in Arabidopsis. Plant Cell **23,** 3463-3481.

Smakowska-Luzan, E., Mott, G.A., Parys, K., Stegmann, M., Howton, T.C., Layeghifard, M., Neuhold, J., Lehner, A., Kong, J., Grunwald, K., Weinberger, N., Satbhai, S.B., Mayer, D., Busch, W., Madalinski, M., Stolt-Bergner, P., Provart, N.J., Mukhtar, M.S., Zipfel, C., Desveaux, D., Guttman, D.S., and Belkhadir, Y. (2018). An extracellular network of Arabidopsis leucine-rich repeat receptor kinases. Nature **553,** 342-346.

Stegmann, M., Zecua-Ramirez, P., Ludwig, C., Lee, H.S., Peterson, B., Nimchuk, Z.L., Belkhadir, Y., and Huckelhoven, R. (2022). RGI-GOLVEN signaling promotes cell surface immune receptor abundance to regulate plant immunity. EMBO Rep **23,** e53281.

Taylor, K.W., Kim, J.G., Su, X.B., Aakre, C.D., Roden, J.A., Adams, C.M., and Mudgett, M.B. (2012). Tomato TFT1 is required for PAMP-triggered immunity and mutations that prevent T3S effector XopN from binding to TFT1 attenuate Xanthomonas virulence. PLoS Pathog **8,** e1002768.

Thor, K., Jiang, S., Michard, E., George, J., Scherzer, S., Huang, S., Dindas, J., Derbyshire, P., Leitao, N., DeFalco, T.A., Koster, P., Hunter, K., Kimura, S., Gronnier, J.,

Stransfeld, L., Kadota, Y., Bucherl, C.A., Charpentier, M., Wrzaczek, M., MacLean, D., Oldroyd, G.E.D., Menke, F.L.H., Roelfsema, M.R.G., Hedrich, R., Feijo, J., and Zipfel, C. (2020). The calcium-permeable channel OSCA1.3 regulates plant stomatal immunity. Nature **585,** 569-573.

Tian, W., Hou, C.C., Ren, Z.J., Wang, C., Zhao, F.G., Dahlbeck, D., Hu, S.P., Zhang, L.Y., Niu, Q., Li, L.G., Staskawicz, B.J., and Luan, S. (2019). A calmodulin-gated calcium channel links pathogen patterns to plant immunity. Nature **572,** 131-+.

Wang, J., Xi, L., Wu, X.N., Konig, S., Rohr, L., Neumann, T., Weber, J., Harter, K., and Schulze, W.X. (2022). PEP7 acts as a peptide ligand for the receptor kinase SIRK1 to regulate aquaporin-mediated water influx and lateral root growth. Mol Plant **15,** 1615-1631.

Wang, Y., Li, J., Hou, S., Wang, X., Li, Y., Ren, D., Chen, S., Tang, X., and Zhou, J.M. (2010). A Pseudomonas syringae ADP-ribosyltransferase inhibits Arabidopsis mitogen-activated protein kinase kinases. Plant Cell **22,** 2033-2044.

Wilton, M., Subramaniam, R., Elmore, J., Felsensteiner, C., Coaker, G., and Desveaux, D. (2010). The type III effector HopF2 Pto targets Arabidopsis RIN4 protein to promote Pseudomonas syringae virulence. Proceedings of the National Academy of Sciences **107,** 2349-2354.

Wu, S., Lu, D., Kabbage, M., Wei, H.L., Swingle, B., Records, A.R., Dickman, M., He, P., and Shan, L. (2011). Bacterial effector HopF2 suppresses arabidopsis innate immunity at the plasma membrane. Mol Plant Microbe Interact **24,** 585-593.

Wu, X.N., Chu, L., Xi, L., Pertl-Obermeyer, H., Li, Z., Sklodowski, K., Sanchez-Rodriguez, C., Obermeyer, G., and Schulze, W.X. (2019). Sucrose-induced Receptor Kinase 1 is Modulated by an Interacting Kinase with Short Extracellular Domain. Mol Cell Proteomics **18,** 1556-1571.

Xiang, T.T., Zong, N., Zou, Y., Wu, Y., Zhang, J., Xing, W.M., Li, Y., Tang, X.Y., Zhu, L.H., Chai, J.J., and Zhou, J.M. (2008). Pseudomonas syringae effector AvrPto blocks innate immunity by targeting receptor kinases. Current Biology **18,** 74-80.

Xu, J., Xie, J., Yan, C.F., Zou, X.Q., Ren, D.T., and Zhang, S.Q. (2014). A chemical genetic approach demonstrates that MPK3/MPK6 activation and NADPH oxidase-mediated oxidative burst are two independent signaling events in plant immunity. Plant Journal **77,** 222-234.

Yang, F., Kimberlin, A.N., Elowsky, C.G., Liu, Y., Gonzalez-Solis, A., Cahoon, E.B., and Alfano, J.R. (2019). A Plant Immune Receptor Degraded by Selective Autophagy. Mol Plant **12,** 113-123.

Yeh, Y.H., Panzeri, D., Kadota, Y., Huang, Y.C., Huang, P.Y., Tao, C.N., Roux, M., Chien,

H.C., Chin, T.C., Chu, P.W., Zipfel, C., and Zimmerli, L. (2016). The Arabidopsis Malectin-Like/LRR-RLK IOS1 Is Critical for BAK1-Dependent and BAK1-Independent Pattern-Triggered Immunity. Plant Cell **28,** 1701-1721.

Zhang, J., Li, W., Xiang, T.T., Liu, Z.X., Laluk, K., Ding, X.J., Zou, Y., Gao, M.H., Zhang, X.J., Chen, S., Mengiste, T., Zhang, Y.L., and Zhou, J.M. (2010). Receptor-like Cytoplasmic Kinases Integrate Signaling from Multiple Plant Immune Receptors and Are Targeted by a Pseudomonas syringae Effector. Cell Host & Microbe **7,** 290-301.

Zhou, J., Wu, S., Chen, X., Liu, C., Sheen, J., Shan, L., and He, P. (2014). The Pseudomonas syringae effector HopF2 suppresses Arabidopsis immunity by targeting BAK1. Plant J **77,** 235-245.

968 **Supporting Information**

969 **Supplemental Figure S1.** Heterologous expression of *QSK1-3xHA* reduces
970 flg22-induced ROS production in *Nicotiana benthamiana.*

971 **Supplemental Figure S2.** T-DNA insertion and expression in *qsk1* mutant.

972 **Supplemental Figure S3.** Phenotype recovery in *qsk1* complementation lines.

973 **Supplemental Figure S4.** *QSK1* overexpression lines are slightly smaller than
974 Col-0 and *qsk1* mutant.

975 **Supplemental Figure S5.** QSK1 localizes at the plasma membrane.

976 **Supplemental Figure S6.** flg22 and elf18 induce the accumulation of *QSK1*
977 transcript.

978 **Supplemental Figure S7.** Pharmacological analyses of FLS2 reduction
979 induced by QSK1.

980 **Supplemental Figure S8.** Pharmacological analyses of FLS2 reduction
981 induced by HopF2$_{Pto}$.

982 **Supplemental Figure S9.** Multidimensional scaling (MDS) plot with self-
983 organizing map (SOM) clustering of genes affected by HopF2$_{Pto}$.

984 **Supplemental Figure S10.** HopF2$_{Pto}$ affects some transcript levels of
985 commonly associated proteins with EFR, FLS2, and RBOHD.

986 **Supplemental Figure S11.** HopF2$_{Pto}$ inhibits PAMP-induced ROS production.

987 **Supplemental Figure S12.** HopF2$_{Pto}$ inhibits PAMP-induced activation of
988 MAPKs.

989 **Supplemental Figure S13.** *Pto* DC3000 *Δhopf2 HopF2$_{Pto}$-HA* grows to the
990 same extent in Col-0 and *qsk1* mutant.

991 **Supplemental Figure S14.** A model of the virulence function of HopF2$_{Pto}$

suppressing PTI and its relationship to QSK1.

Supplemental Figure S15. *lrr1* and *rkl1* mutants have higher ROS production in response to flg22, elf18, and pep1.

Supplemental Figure S16. SIRK1 and PEP7 do not affect PAMP-induced ROS production.

Supplemental Methods S1. Additional methods.

Supplemental Data Set S1_1. FLS2-associated proteins.

Supplemental Data Set S1_2. EFR-associated proteins.

Supplemental Data Set S1_3. RBOHD-associated proteins.

Supplemental Data Set S1_4. Commonly associated proteins with FLS2, EFR, and RBOHD.

Supplemental Data Set S2_1. Peptide counts of QSK1 in FLS2-GFP IP analysis.

Supplemental Data Set S2_2. Peptide counts of QSK1 in EFR-GFP IP analysis.

Supplemental Data Set S2_3. Peptide counts of QSK1 in FLAG-RBOHD IP analysis.

Supplemental Data Set S3_1. Enrichment score of HopF2$_{Pto}$ interactors in Quantitative Interactor Screening with Next-Generation Sequencing (QIS-Seq).

Supplemental Data Set S3_2. In planta proximity-dependent biotin identification (BioID) of HopF2$_{Pto}$ associated proteins

Supplemental Data Set S4_1. Normalized expression values of genes in Arabidopsis seedlings of Col-0 or *pDEX:HopF2$_{Pto}$-HA* lines treated with DMSO

or DEX.

Supplemental Data Set S4_2. Up-regulated genes by DEX treatment compared to DMSO treatment in Col-0 (log2 fold change ≥ 1, FDR ≤ 0.05).

Supplemental Data Set S4_3. Down-regulated genes by DEX treatment compared to DMSO treatment in Col-0 (log2 fold change ≤ -1, FDR ≤ 0.05).

Supplemental Data Set S4_4. Up-regulated genes by the expression of *HopF2*$_{Pto}$ (*pDEX:HopF2*$_{Pto}$*+DEX* vs Col-0+DEX) (log2 fold change ≥ 1, FDR ≤ 0.05).

Supplemental Data Set S4_5. Down-regulated genes by the expression of *HopF2*$_{Pto}$ (*pDEX:HopF2*$_{Pto}$+DEX vs Col-0+DEX) (log2 fold change ≤ -1, FDR ≤ 0.05).

Supplemental Data Set S4_6. Up-regulated genes by DEX treatment in *pDEX:HopF2*$_{Pto}$*-HA* line (*pDEX:HopF2*$_{Pto}$+DEX vs *pDEX:HopF2*$_{Pto}$+DMSO) (log2 fold change ≥ 1, FDR ≤ 0.05).

Supplemental Data Set S4_7. Down-regulated genes by DEX treatment in *pDEX:HopF2*$_{Pto}$*-HA* line (*pDEX:HopF2*$_{Pto}$+DEX vs *pDEX:HopF2*$_{Pto}$+DMSO) (log2 fold change ≤ -1, FDR ≤ 0.05).

Supplemental Data Set S5_1. Gene ontology (GO) enrichment analysis of the up-regulated genes by HopF2$_{Pto}$

Supplemental Data Set S5_2. Gene ontology (GO) enrichment analysis of the down-regulated genes by HopF2$_{Pto}$

Supplemental Data Set S5_3. Gene ontology (GO) enrichment analysis of the genes in the cluster 1

Supplemental Data Set S5_4. Gene ontology (GO) enrichment analysis of the

genes in the cluster 2

Supplemental Data Set S6. Genes in SOM clusters.

Supplemental Data Set S7. Results of statistical analysis.

Supplemental Data Set S8. Primers used in this paper.

A

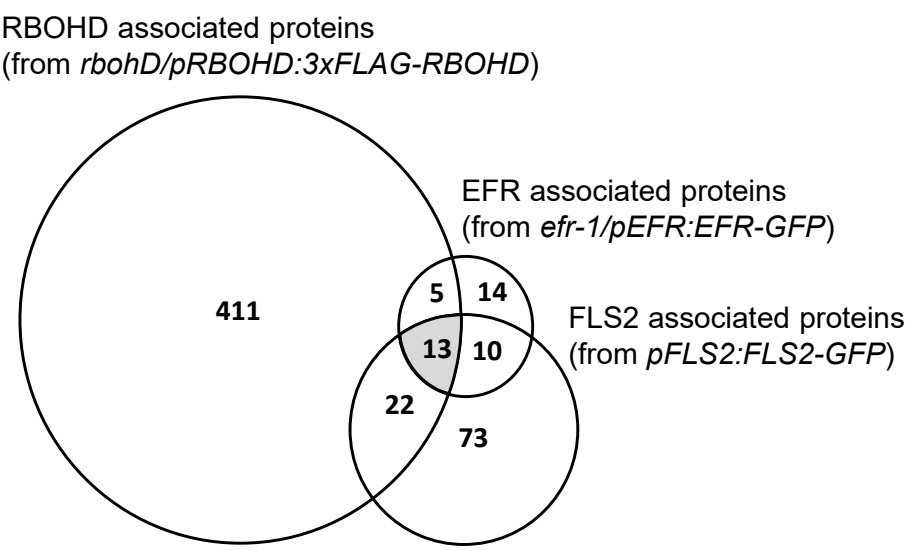

B The common associated proteins with EFR, FLS2, and RBOHD

AGI code	Description
AT4G33430*	BRI1-associated receptor kinase (BAK1)
AT1G51800*	Leucine-rich repeat protein kinase family protein (IOS1)
AT3G02880**	Leucine-rich repeat protein kinase family protein (QSK1)
AT2G39010	Plasma membrane intrinsic protein 2E (PIP2E)
AT4G29900*, **	Autoinhibited Ca^{2+}-ATPase 10 (ACA10)
AT3G09740**	Syntaxin of plants 71 (SYP71)
AT1G69840**	Hypersensitive Induced Reaction 1(HIR1)
AT5G62740**	Hypersensitive Induced Reaction 4 (HIR4)
AT3G07160	Glucan synthase-like 10 (GSL10)
AT4G35790	Phospholipase D delta (PLD DELTA)
AT5G47910*	Respiratory burst oxidase homologue D (RBOHD)
AT3G61260**	Remorin (REM1.2)
AT5G62670	H^+-ATPase 11 (AHA11)

Figure 1.
Commonly associated proteins with EFR, FLS2, and RBOHD in *Arabidopsis thaliana.* **A)** Comparison of candidate-associated proteins with EFR, FLS2, and RBOHD identified by co-immunoprecipitation. The Venn diagram illustrates candidate-associated proteins identified by IP of EFR-GFP, FLS2-GFP or 3xFLAG-RBOHD from Arabidopsis seedlings of *efr-1/pEFR:EFR-GFP* (Kadota et al., 2014), *fpFLS2:FLS2-GFP*, or *rbohD/pRBOHD:3×FLAG-gRBOHD* (Goto et al., 2023). The protein list is shown in Supplemental Data Set S1. **B)** The list of commonly associated proteins with EFR, FLS2, and RBOHD. An asterisk indicates the known components of the PRR complex, and the double asterisks indicate proteins accumulate in detergent-resistant membrane compartments in response to flg22 (Keinath et al., 2010).

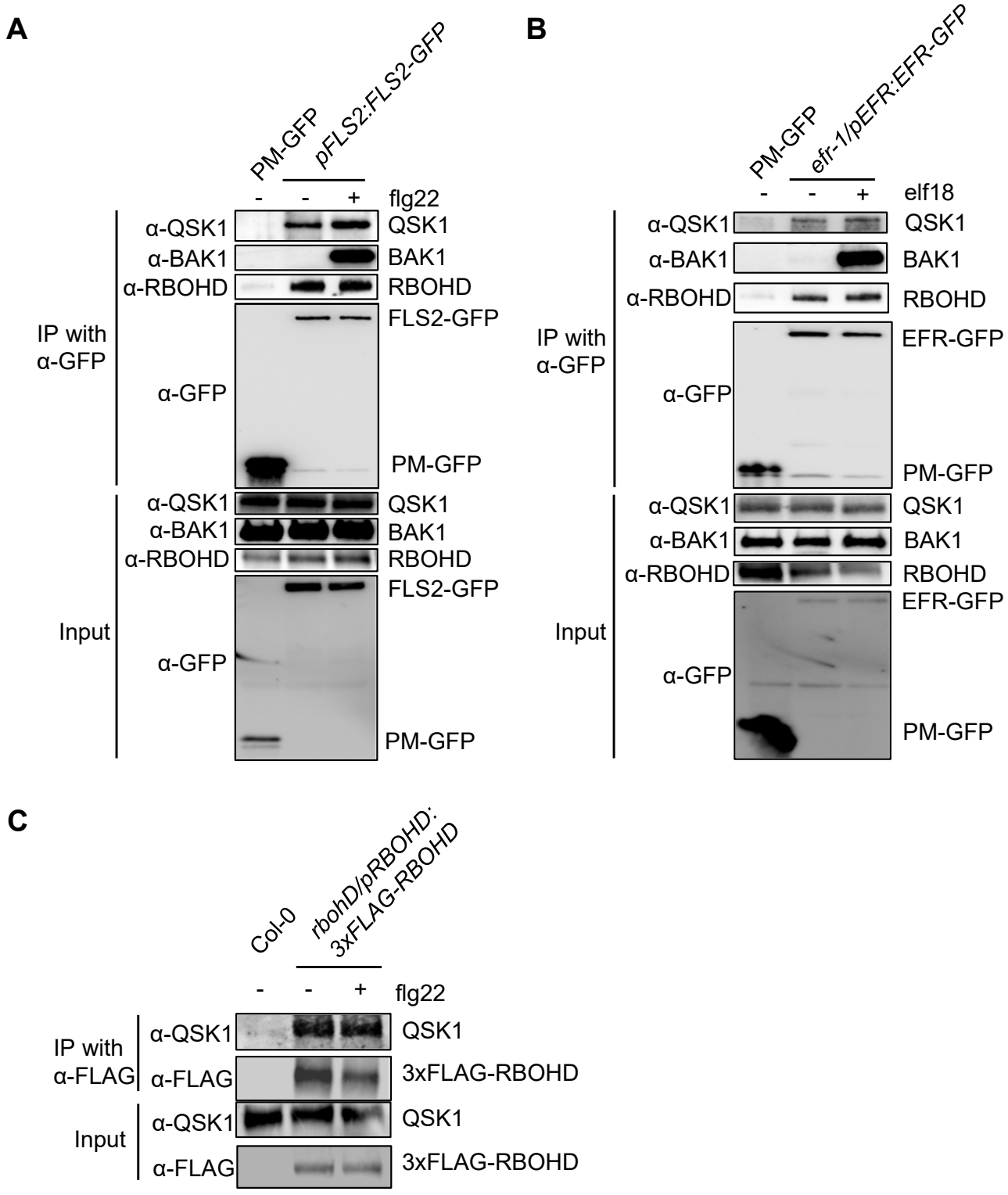

Figure 2.
QSK1 forms a stable complex with FLS2, EFR, and RBOHD in Arabidopsis thaliana. **A and B)** Two-week-old Arabidopsis seedlings of *pFLS2:FLS2-GFP*, *efr-1/pEFR:EFR-GFP*, or PM-GFP (*p35S:LTI6b-GFP*) were treated with or without 1 μM flg22 or 1 μM flg22 for 10 min. Total proteins (input) were immunoprecipitated with α-GFP magnetic beads, followed by immunoblotting with α-GFP, α-QSK1, α-BAK1, and α-RBOHD antibodies. LTI6b, a known plasma membrane protein was used as a control to illustrate that QSK1, RBOHD, and BAK1 do not associate with GFP at the plasma membrane. **C)** Two-week-old Arabidopsis seedlings of rbohD/pRBOHD:3xFLAG-RBOHD or Col-0 were treated with or without 1 μM flg22 for 10 min, and the total proteins were immunoprecipitated with α-FLAG magnetic beads followed by immunoblotting with α-FLAG and α-QSK1 antibodies. Col-0 plants were used as a control to illustrate that QSK1 does not associate with α-FLAG nonspecifically. All the experiments were repeated three times with similar results.

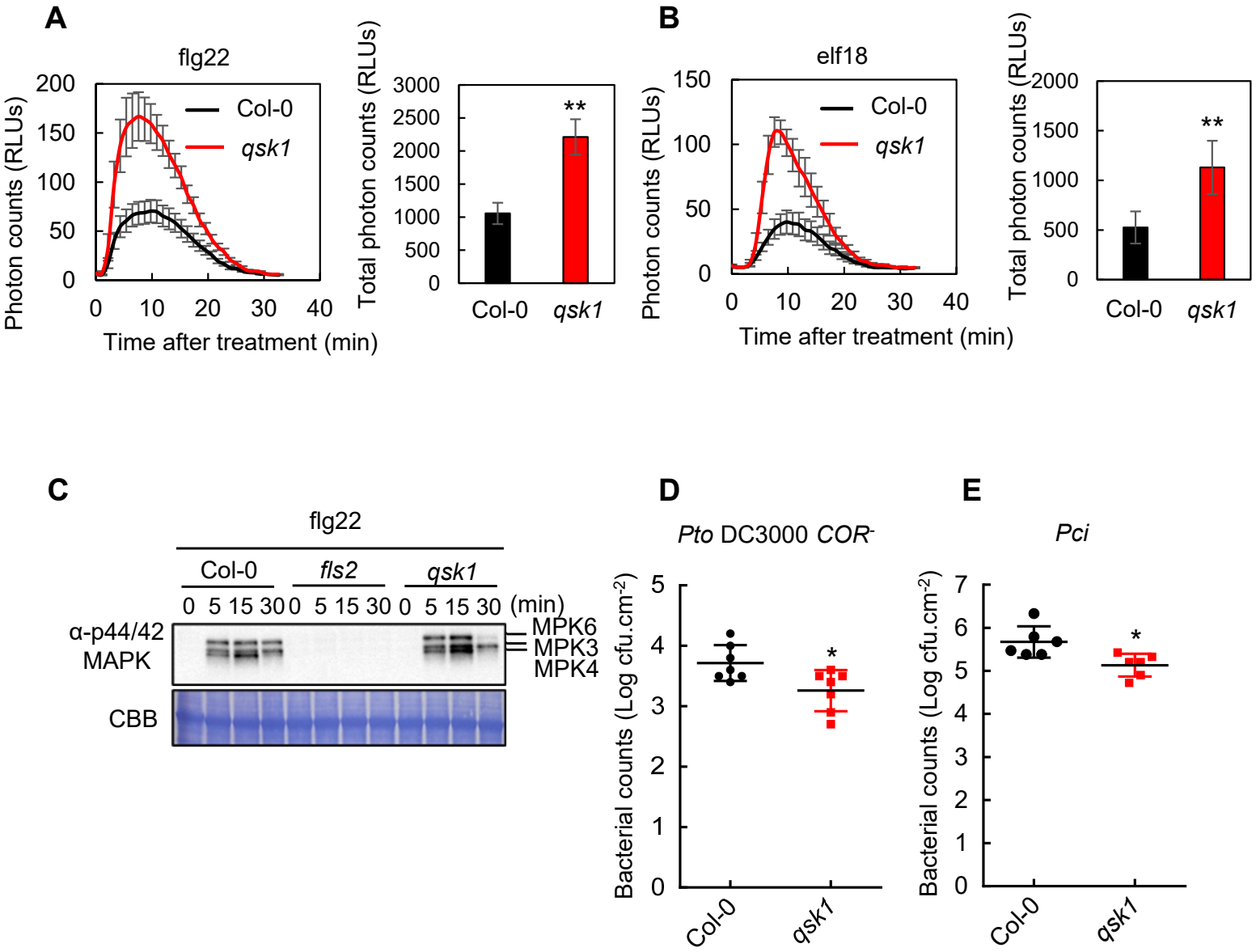

Figure 3.
Arabidopsis *qsk1* mutant shows enhanced PTI responses compared to Col-0. **A and B)** *qsk1* mutant has enhanced ROS production following treatment with flg22 and elf18. Eight leaf discs from four- to five-week-old Arabidopsis plants were treated with 1 μM flg22 (**A**) or 1 μM elf18 (**B**), and time-course (left) and the total amount (right) of ROS production was measured by a luminol-based assay. Values are mean ± standard error (SE) (n=8). An asterisk indicates significant differences (Student's t-test, $^{*}p \leq 0.05$). **C)** *qsk1* mutant induced enhanced MAPKs activation following treatment with flg22. Ten-day-old Arabidopsis seedlings were treated with 1 μM flg22 and phosphorylated MAPKs were detected on immunoblotting with α-phospho-p44/42 MAPK (Erk1/2) (Thr202/Tyr204) antibody. Equal loading of protein samples is shown by Coomassie Brilliant Blue (CBB) staining. **D and E**) *qsk1* mutant was more resistant to bacteria. *Pseudomonas syringae* pv. *tomato* (*Pto*) DC3000 lacking the toxin coronatine (*COR*$^{-}$) (**D**) or *Pseudomonas syringae* pv. *cilantro* (*Pci*) 0788-9 (**E**) were sprayed onto leaf surfaces of six-week-old soil-grown Arabidopsis plants at a concentration of $1x10^5$ cfu (colony-forming units)/mL. Three-day post spray-inoculation, leaves were harvested to determine bacterial growth. Data are means ± SE of 6 replicates. An asterisk indicates significant differences (Student's t-test, $^{*}p \leq 0.05$). All the experiments were repeated three times with similar results.

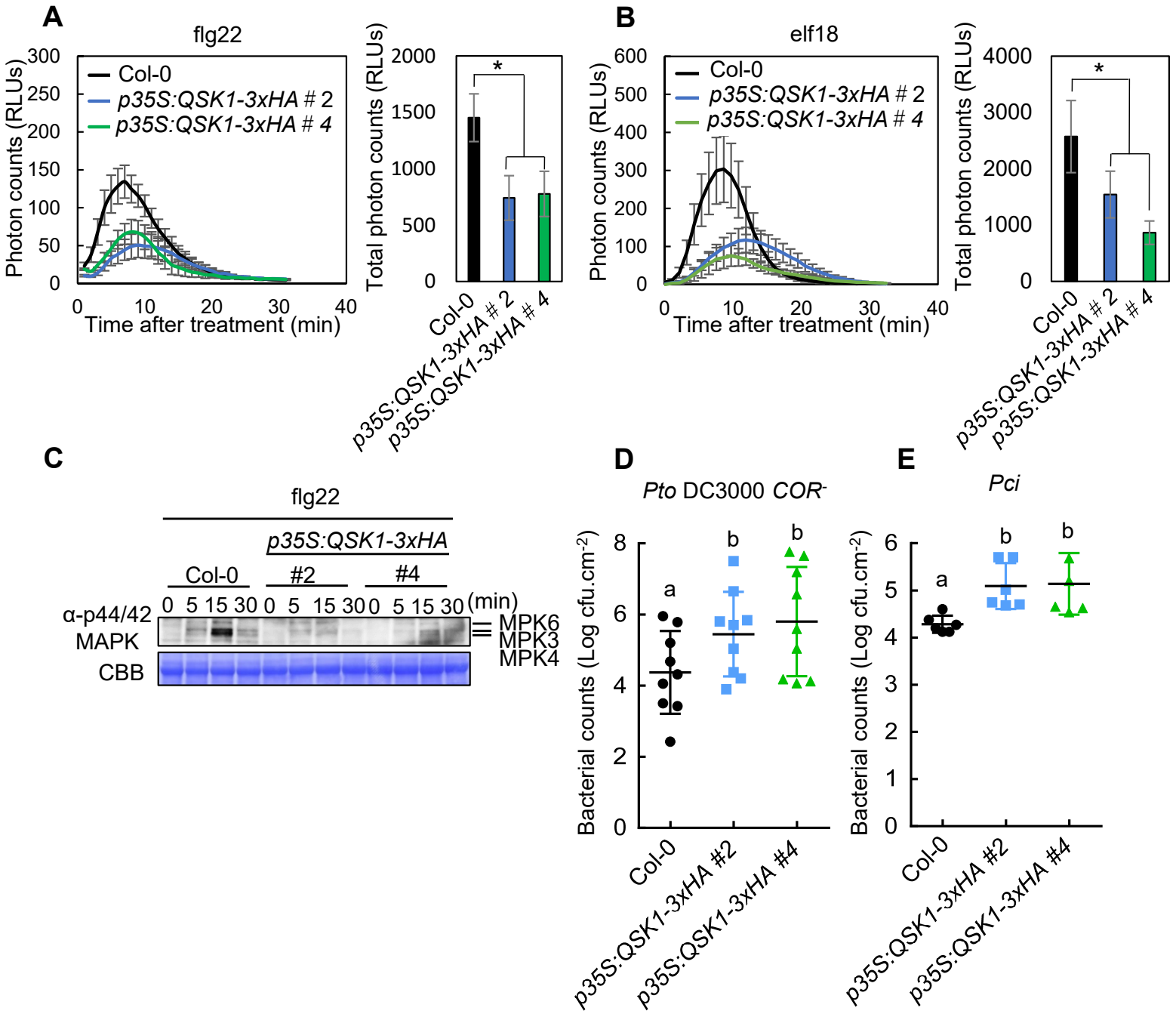

Figure 4.
Arabidopsis *QSK1* over expression lines (*p35S:QSK1 ×HA* QSK1) have reduced PTI responses compared to Col-0. **A and B)** *p35S:QSK1 ×HA* lines showed reduced ROS production in response to flg22 and elf18. Eight seven-day-old Arabidopsis seedlings were treated with 1 µM flg22 (**A**) or 1 µM elf18 (**B**), and time-course (left) and the total amount (right) of ROS production was measured by a luminol-based assay. Values are mean ± SE (n=8). An asterisk indicates significant differences (Student's t-test, $^{*}p \leq 0.05$). **C)** *p35S:QSK1 ×HA* lines showed reduced MAPKs activation in response to flg22. Ten-day-old Arabidopsis seedlings were treated with 1 µM flg22 and phosphorylated MAPKs were detected on immunoblotting with α-phospho-p44/42 MAPK (Erk1/2) (Thr202/Tyr204) antibody. Equal loading of protein samples is shown by CBB staining. **D and E)** *p35S:QSK1 ×HA* lines were more susceptible to bacteria. *Pto* DC3000 *COR*$^{-}$ (**D**) or *Pci* (**E**) were sprayed onto leaf surfaces of six-week-old soil-grown Arabidopsis plants at a concentration of $1x10^5$ cfu/mL. Three-day post spray-inoculation, leaves were harvested to determine bacterial growth. Data are means ± SE of 6 replicates. Different letters indicate significantly different values at $p \leq 0.05$ (one-way ANOVA, Tukey post hoc test). All the experiments were repeated three times with similar results.

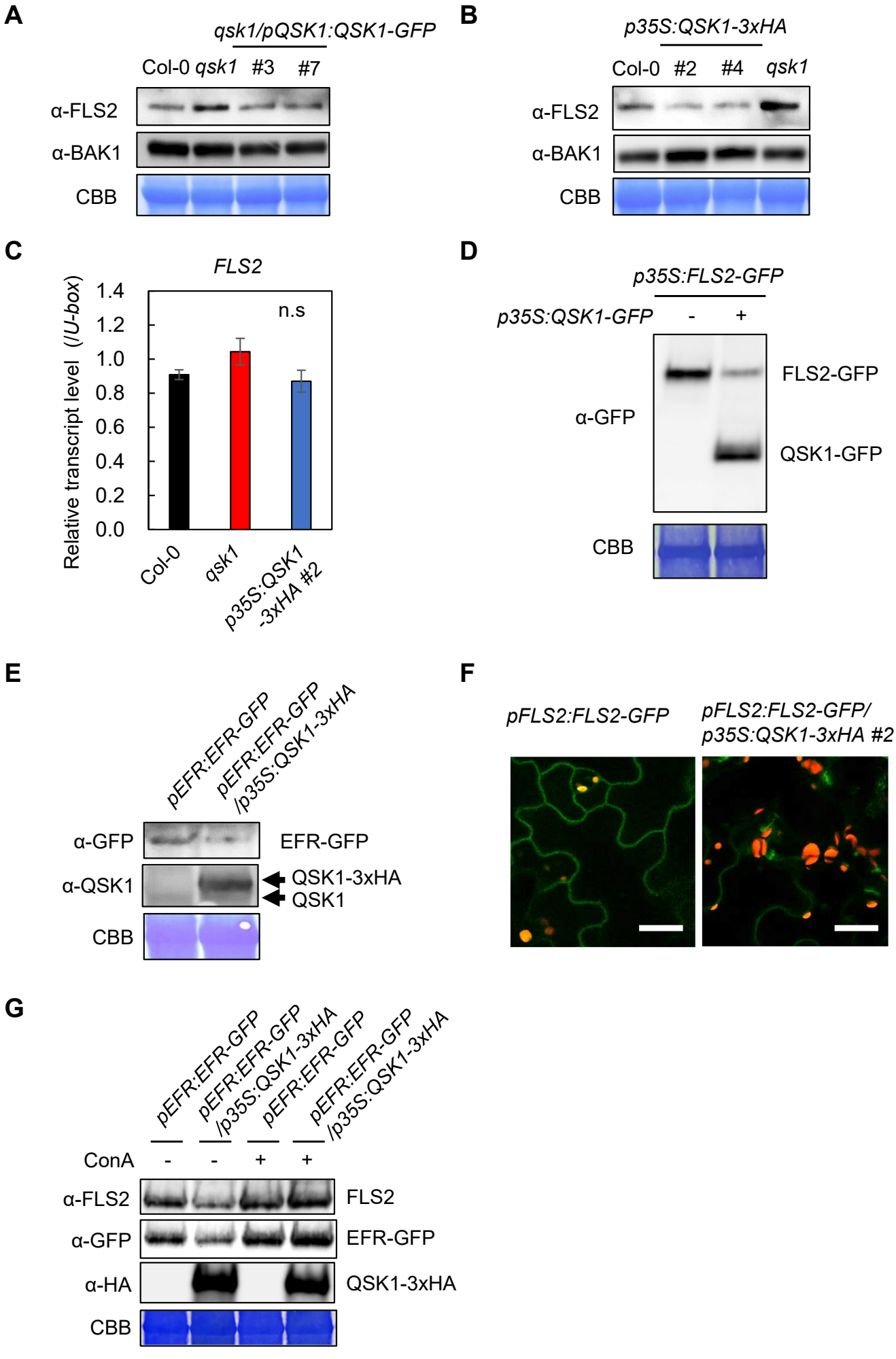

Figure 5.

QSK1 negatively regulates FLS2 and EFR accumulation. **A)** FLS2 protein accumulates more in *qsk1* mutant than in Col-0 and the complementation lines (*qsk1/pQSK1:QSK1-GFP*). **B)** FLS2 protein accumulates less in *p35S:QSK1 ×HA* lines than in Col-0. FLS2 and BAK1 protein levels of two-week-old Arabidopsis seedlings were measured by immunoblotting with α-FLS2 and α-BAK1 antibodies. Equal loading of protein samples is shown by CBB staining. **C)** FLS2 transcript levels are not changed in Col-0, *qsk1* mutant, and *p35S:QSK1 ×HA* lines. Transcript levels of *FLS2* in two-week-old Arabidopsis seedlings were measured by RT-qPCR after normalization to the *U-box* housekeeping gene transcript (*At5g15400*). Values are mean ± SE of three biological replicates. There are no significant differences at $p \leq 0.05$ (one-way ANOVA, Turkey's *post hoc* test). **D**) The expression of *QSK1-GFP* reduces FLS2-GFP protein levels in *Nicotiana benthamiana.* FLS2-GFP and QSK1-GFP proteins were transiently expressed under the control of *p35S* promoter and their protein levels were measured three days after agroinfiltration by immunoblotting with α-GFP antibodies. Agrobacterium concentration (OD600=0.6) was adjusted with empty Agrobacterium. **E)** QSK1 reduces EFR protein levels. Protein levels of EFR-GFP and QSK1 in two-week-old Arabidopsis seedlings of *pEFR:EFR-GFP* and *pEFR:EFR-GFP*/*p35S:QSK1-3xHA* were measured by immunoblotting with α-GFP antibodies. **F)** QSK1 reduces FLS2 protein accumulation at the plasma membrane. The localization of FLS2-GFP in cotyledons of ten-day-old seedlings of *pFLS2:FLS2-GFP* line and *pFLS2:FLS2-GFP/p35S:QSK1-3xHA#2* line were observed by confocal microscopy. The white bars represent 30 μm. **G)** Concanamycin A (ConA) suppresses QSK1-mediated PRR reduction. Two-week-old Arabidopsis seedlings of *pEFR:EFR-GFP* and *p35S:QSK1-3xHA*/*pEFR:EFR-GFP* lines were treated with or without 1 μM ConA for 10 h. The protein levels of FLS2, EFR-GFP, and QSK1-3xHA were measured by immunoblotting. Equal loading of protein samples is shown by CBB staining. All the experiments were repeated three times with similar results.

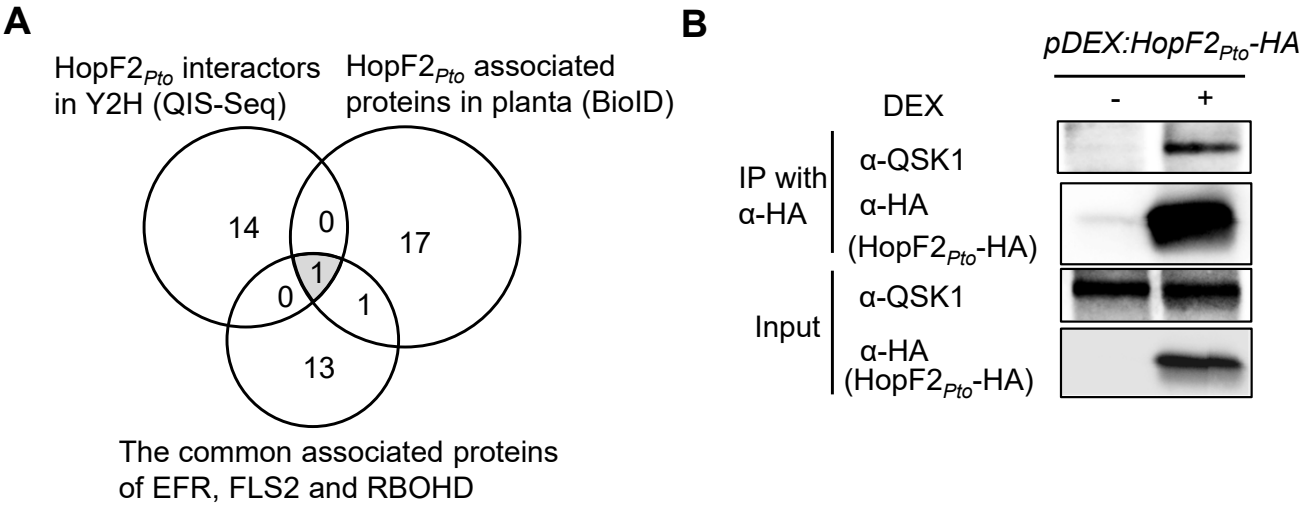

Figure 6.

HopF2$_{Pto}$ associates with QSK1 and reduces FLS2 protein level. **A)** Comparison of candidate interactors of HopF2$_{Pto}$ and the commonly associated proteins with EFR, FLS2, and RBOHD. The Venn diagram illustrates candidate HopF2$_{Pto}$ interactors identified by yeast two-hybrid screening coupled with next-generation sequencing (QIS-Seq) and by proximity-dependent biotin identification (BioID) in planta (Khan et al., 2018) with the commonly associated proteins with EFR, FLS2, and RBOHD identified in this study. **B)** HopF2$_{Pto}$ associates with QSK1 *in vivo*. Two-week-old Arabidopsis seedlings of *pDEX:HopF2$_{Pto}$-HA* were treated with or without 30 μM dexamethasone (DEX) for 24 h. Total proteins (input) were immunoprecipitated with α-HA magnetic beads followed by immunoblotting with α-HA and α-QSK antibodies. **C and D**) HopF2$_{Pto}$ specifically reduced FLS2 protein accumulation. Two-week-old Arabidopsis seedlings of *pDEX:HopF2$_{Pto}$-HA* were treated with or without 30 μM DEX and FLS2, RBOHD, BAK1, QSK1, and HopF2$_{Pto}$-HA protein levels were measured by immunoblotting. Equal loading of protein samples is shown by CBB staining. **E)** HopF2$_{Pto}$ reduced FLS2 protein accumulation at the plasma membrane. Ten-day-old seedlings of *pFLS2:FLS2-GFP/ pDEX:HopF2$_{Pto}$-HA* line were treated with or without 30 μM DEX for 24 h and the localization of FLS2-GFP in cotyledons was observed by confocal microscopy. The white bar represents 50 μm. All the experiments were repeated three times with similar results.

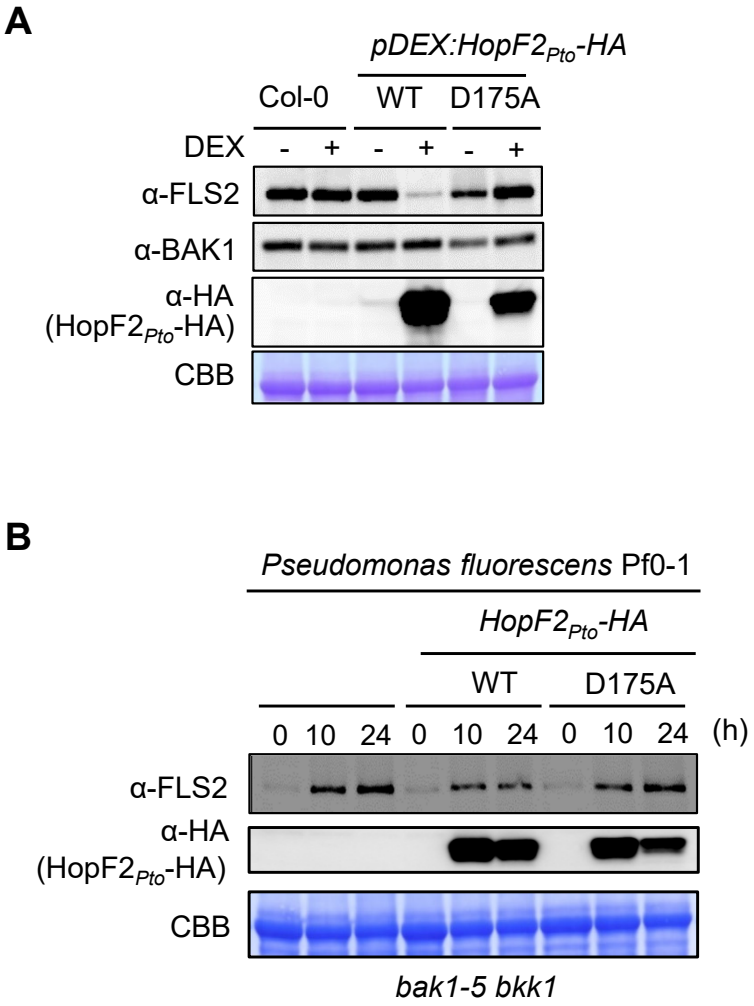

Figure 7.
Mono ADP ribosylation (MARylation) activity of HopF2$_{Pto}$ is required for the FLS2 elimination. **A)** The catalytic residue D175 for MARylation activity in HopF2$_{Pto}$ is required for the inhibition of FLS2 accumulation. Two-week-old Arabidopsis seedlings of *pDEX:HopF2$_{Pto}$-HA* and *pDEX:HopF2$_{Pto}$* (D175A)-*HA* were treated with 30 μM DEX for 24 h and FLS2, BAK1, and HopF2$_{Pto}$ -HA protein levels were measured by immunoblotting. **B)** HopF2$_{Pto}$ inhibits FLS2 protein accumulation during infection. Immunoblotting detecting FLS2 and HopF2$_{Pto}$-HA in Col-0 during bacterial infection after syringe inoculation with *Pseudomonas fluorescens* Pf0-1, *P. fluorescens* Pf0-1 *HopF2$_{Pto}$-HA*, or *P. fluorescens* Pf0-1 *HopF2$_{Pto}$* (D175A)-*HA*. All the experiments were repeated three times with similar results.

A

Accession	Col-0 + DMSO	Col-0 + DEX	*pDEX:HopF2$_{Pto}$* + DMSO	*pDEX:HopF2$_{Pto}$* + DEX	FDR
FLS2	101.0	106.8	100.0	19.5	1.15E-24
LORE	114.9	137.3	100.0	23.1	1.01E-27
CARD1	103.1	139.3	100.0	43.5	1.02E-16
RDA2	116.6	169.6	100.0	30.2	2.07E-09
MIK2	148.1	239.6	100.0	13.7	4.64E-90
WAK1	156.3	369.2	100.0	22.8	3.27E-24
WAK2	121.8	303.4	100.0	17.4	1.79E-20
EFR	150.0	233.6	100.0	87.5	n.s
PEPR1	92.4	83.5	100.0	87.2	n.s
LYK5	91.4	268.9	100.0	146.3	n.s
RLP23	109.8	171.6	100.0	81.4	n.s
LYP2	130.6	104.2	100.0	74.2	n.s
RBPG1	65.4	140.0	100.0	117.4	n.s

B

Accession	Col-0 + DMSO	Col-0 + DEX	*pDEX:HopF2$_{Pto}$* + DMSO	*pDEX:HopF2$_{Pto}$* + DEX	FDR
PROSCOOP1	71.5	78.0	100.0	43.6	1.21E-10
PROSCOOP4	185.1	408.8	100.0	27.9	4.88E-28
PROSCOOP6	144.1	217.0	100.0	25.7	2.56E-50
PROSCOOP7	137.1	133.6	100.0	5.3	1.80E-25
PROSCOOP8	311.6	440.0	100.0	0.0	9.82E-107
PROSCOOP10	126.7	126.4	100.0	9.6	2.68E-121
PROSCOOP11	130.5	132.6	100.0	20.7	5.70E-20
PROSCOOP12	211.4	364.1	100.0	10.8	1.54E-80
PROSCOOP13	93.8	85.0	100.0	33.1	1.55E-26
PROSCOOP14	121.8	224.8	100.0	18.2	1.33E-42
PROSCOOP20	147.9	295.0	100.0	28.8	4.88E-15
PROSCOOP23	192.5	590.1	100.0	6.5	7.41E-31
PROPEP1	73.6	88.5	100.0	60.7	n.s
PROPEP6	62.6	55.1	100.0	115.4	n.s
PROPEP4	84.8	84.0	100.0	68.2	2.38E-02
PROPEP5	90.4	97.6	100.0	42.3	1.33E-12
PIP1	135.4	295.5	100.0	81.7	n.s

Figure 8.
HopF2$_{Pto}$ reduces transcript levels of *PRRs* and *PROSCOOPs*. Transcript levels of *PRRs* (**A**), *PROSCOOPs*, *PROPEPs,* and *PIP1* (**B**) were measured by RNA-seq in two-week-old seedlings of Col-0 and *pDEX:HopF2$_{Pto}$-HA* after treatment with 30 µM DEX for 24 h. The relative expression values of the genes are shown compared to the "*pDEX:HopF2$_{Pto}$* + DMSO" control. The FDR values between "*pDEX:HopF2$_{Pto}$* + DMSO" and "*pDEX:HopF2$_{Pto}$* + DEX" are shown. Grey boxes in the heat map indicate no statistically significant difference at FDR ≤ 0.05.

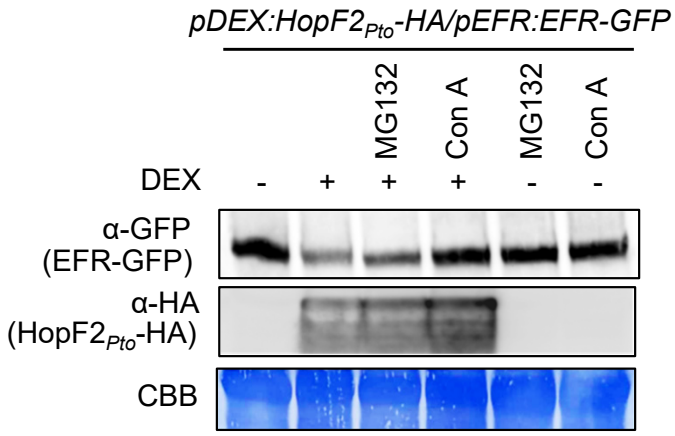

Figure 9.
Con A inhibits HopF2$_{Pto}$ -mediated reduction of EFR expression. Two-week-old Arabidopsis seedlings of *pDEX:HopF2$_{Pto}$-HA*/*pEFR:EFR-GFP* were treated with or without 30 μM DEX for 24 h, followed by the treatment with DMSO, 100 μM MG132, or 1 μM ConA for 10 h. The protein levels of EFR-GFP and HopF2$_{Pto}$-HA were measured by immunoblotting with α-GFP and α-HA antibodies. Equal loading of protein samples is shown by CBB staining. This experiment was repeated three times with similar results.

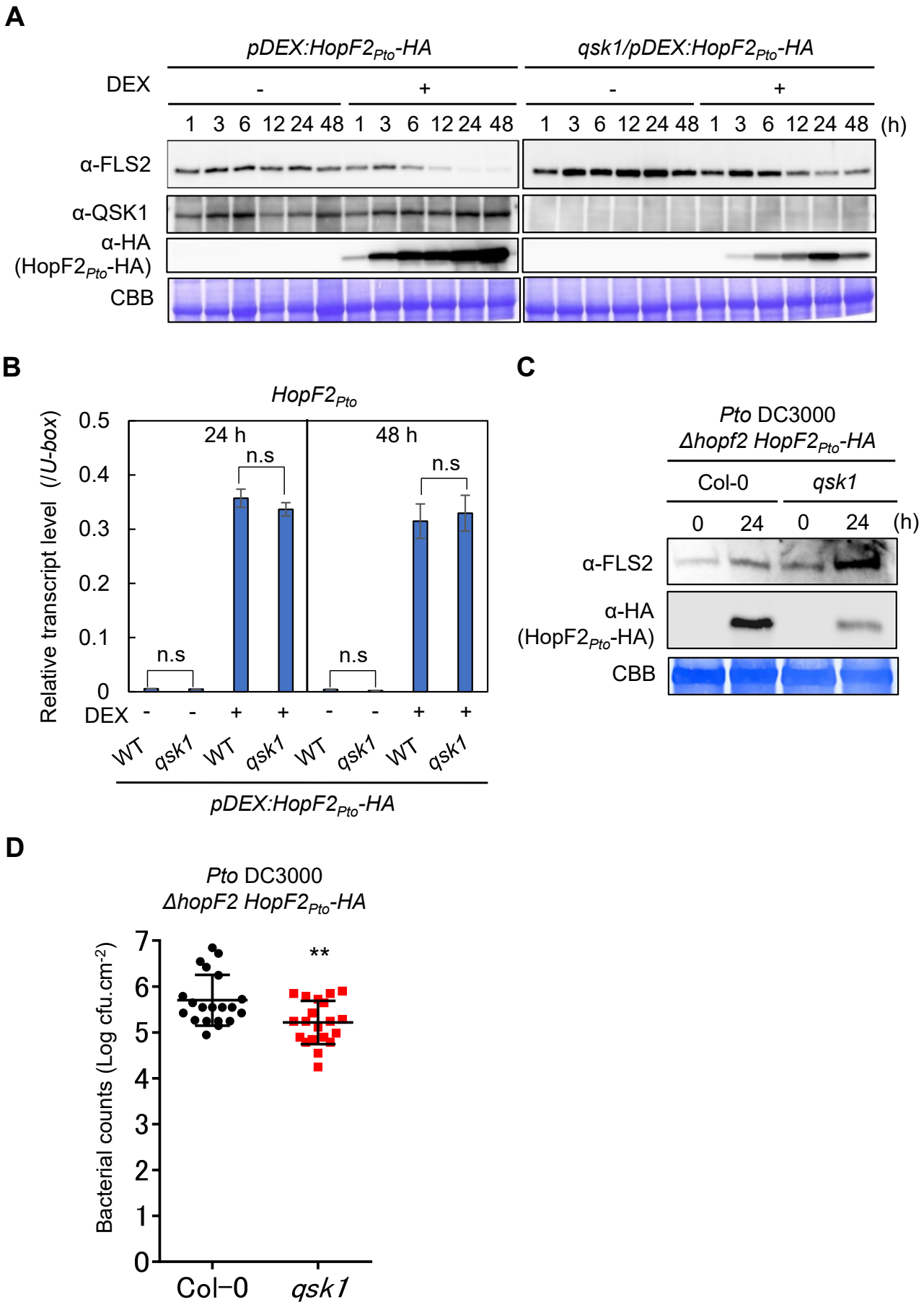

Figure 10.

HopF2$_{Pto}$ requires QSK1 for its protein accumulation and function.

A) HopF2$_{Pto}$ requires QSK1 for its protein accumulation and suppression of FLS2 accumulation. Two-week-old Arabidopsis seedlings of *pDEX:HopF2$_{Pto}$-HA* and qsk1/*pDEX:HopF2$_{Pto}$-HA* were treated with 30 μM DEX for 1, 3, 6, 12, 24 and 48 h and FLS2, QSK1, and HopF2$_{Pto}$-HA protein levels were measured by immunoblotting with α-FLS2, α-QSK1, and α-HA antibodies. **B)** QSK1 does not affect *HopF2$_{Pto}$* transcript levels. Transcript levels of *HopF2$_{Pto}$-HA* in two-week-old Arabidopsis seedlings of *pDEX:HopF2$_{Pto}$-HA* and *qsk1*/*pDEX:HopF2$_{Pto}$-HA* treated with 30 μM DEX for 24 h and 48 h were measured by RT-qPCR after normalization to the *U-box* housekeeping gene transcript (*At5g15400*). erisks indicate significant differences (Student's t-test, $^{**}p \leq 0.01$). All the experiments were repValues are mean ± SE of three biological replicates. There are no significant differences at $p \leq 0.05$ between the two lines with or without treatment with DEX (Student's t-test). **C)** HopF2$_{Pto}$ requires QSK1 during infection. Five-week-old Arabidopsis Col-0 and *qsk1* mutant were syringe-inoculated with *Pto* DC3000 *Δhopf2 HopF2$_{Pto}$-HA* (inoculum: 10^8 cfu/ml). Immunoblotting detecting FLS2 and HopF2$_{Pto}$-HA at 1 d post-infection (dpi). The similar bacterial population at 1 dpi was confirmed by the bacterial growth assay shown in Supplemental Figure S13. **D)** *qsk1* mutant is more resistant against *Pto* DC3000 *Δhopf2 HopF2$_{Pto}$-HA*. *Pto* DC3000 *Δhopf2 HopF2$_{Pto}$-HA* were sprayed onto leaf surfaces of five-week-old soil-grown Arabidopsis plants at a concentration of $1x10^5$ cfu/mL. Data are means ± standard deviation of 20 replicates. The central horizontal line indicates the mean value. Asteated three times with similar results.

Parsed Citations

Aryal, B., Xia, J., Hu, Z., Stumpe, M., Tsering, T., Liu, J., Huynh, J., Fukao, Y., Glockner, N., Huang, H.Y., Sancho-Andres, G., Pakula, K., Ziegler, J., Gorzolka, K., Zwiewka, M., Nodzynski, T., Harter, K., Sanchez-Rodriguez, C., Jasinski, M., Rosahl, S., and Geisler, M.M. (2023). An LRR receptor kinase controls ABC transporter substrate preferences during plant growth-defense decisions. Curr Biol 33, 2008-2023 e2008.

Google Scholar: Author Only Title Only Author and Title

Beck, M., Zhou, J., Faulkner, C., MacLean, D., and Robatzek, S. (2012). Spatio-temporal cellular dynamics of the Arabidopsis flagellin receptor reveal activation status-dependent endosomal sorting. Plant Cell 24, 4205-4219.

Google Scholar: Author Only Title Only Author and Title

Boudsocq, M., Willmann, M.R., McCormack, M., Lee, H., Shan, L.B., He, P., Bush, J., Cheng, S.H., and Sheen, J. (2010). Differential innate immune signalling via Ca2+ sensor protein kinases. Nature 464, 418-U116.

Google Scholar: Author Only Title Only Author and Title

Chen, X., Wang, T., Rehman, A.U., Wang, Y., Qi, J., Li, Z., Song, C., Wang, B., Yang, S., and Gong, Z. (2021). Arabidopsis U-box E3 ubiquitin ligase PUB11 negatively regulates drought tolerance by degrading the receptor-like protein kinases LRR1 and KIN7. J Integr Plant Biol 63, 494-509.

Google Scholar: Author Only Title Only Author and Title

Cheng, W., Munkvold, K.R., Gao, H.S., Mathieu, J., Schwizer, S., Wang, S., Yan, Y.B., Wang, J.J., Martin, G.B., and Chai, J.J. (2011). Structural Analysis of Pseudomonas syringae AvrPtoB Bound to Host BAK1 Reveals Two Similar Kinase-Interacting Domains in a Type III Effector. Cell Host & Microbe 10, 616-626.

Google Scholar: Author Only Title Only Author and Title

Chinchilla, D., Bauer, Z., Regenass, M., Boller, T., and Felix, G. (2006). The Arabidopsis receptor kinase FLS2 binds flg22 and determines the specificity of flagellin perception. Plant Cell 18, 465-476.

Google Scholar: Author Only Title Only Author and Title

Chinchilla, D., Zipfel, C., Robatzek, S., Kemmerling, B., Nurnberger, T., Jones, J.D., Felix, G., and Boller, T. (2007). A flagellin-induced complex of the receptor FLS2 and BAK1 initiates plant defence. Nature 448, 497-500.

Google Scholar: Author Only Title Only Author and Title

Dettmer, J., Hong-Hermesdorf, A., Stierhof, Y.D., and Schumacher, K. (2006). Vacuolar H+-ATPase activity is required for endocytic and secretory trafficking in Arabidopsis. Plant Cell 18, 715-730.

Google Scholar: Author Only Title Only Author and Title

Dou, D.L., and Zhou, J.M. (2012). Phytopathogen Effectors Subverting Host Immunity: Different Foes, Similar Battleground. Cell Host & Microbe 12, 484-495.

Google Scholar: Author Only Title Only Author and Title

Feng, F., Yang, F., Rong, W., Wu, X.G., Zhang, J., Chen, S., He, C.Z., and Zhou, J.M. (2012). A Xanthomonas uridine 5 '-monophosphate transferase inhibits plant immune kinases. Nature 485, 114-U149.

Google Scholar: Author Only Title Only Author and Title

Frei dit Frey, N., Mbengue, M., Kwaaitaal, M., Nitsch, L., Altenbach, D., Haweker, H., Lozano-Duran, R., Njo, M.F., Beeckman, T., Huettel, B., Borst, J.W., Panstruga, R., and Robatzek, S. (2012). Plasma membrane calcium ATPases are important components of receptor-mediated signaling in plant immune responses and development. Plant Physiology 159, 798-+.

Google Scholar: Author Only Title Only Author and Title

Fu, Z.Q., Guo, M., Jeong, B.R., Tian, F., Elthon, T.E., Cerny, R.L., Staiger, D., and Alfano, J.R. (2007). A type III effector ADP-ribosylates RNA-binding proteins and quells plant immunity. Nature 447, 284-288.

Google Scholar: Author Only Title Only Author and Title

Gimenez-Ibanez, S., Hann, D.R., Ntoukakls, V., Petutschnig, E., Lipka, V., and Rathjen, J.P. (2009). AvrPtoB Targets the LysM Receptor Kinase CERK1 to Promote Bacterial Virulence on Plants. Current Biology 19, 423-429.

Google Scholar: Author Only Title Only Author and Title

Goehre, V., Spallek, T., Haeweker, H., Mersmann, S., Mentzel, T., Boller, T., de Torres, M., Mansfield, J.W., and Robatzek, S. (2008). Plant Pattern-Recognition Receptor FLS2 Is Directed for Degradation by the Bacterial Ubiquitin Ligase AvrPtoB. Current Biology 18, 1824-1832.

Google Scholar: Author Only Title Only Author and Title

Goto, Y., Maki, N., Ichihashi, Y., Kitazawa, D., Igarashi, D., Kadota, Y., and Shirasu, K. (2020). Exogenous Treatment with Glutamate Induces Immune Responses in Arabidopsis. Mol Plant Microbe Interact 33, 474-487.

Google Scholar: Author Only Title Only Author and Title

Goto, Y., Maki, N., Sklenar, J., Derbyshire, P., Menke, F.L.H., Zipfel, C., Kadota, Y., and Shirasu, K. (2023). The phagocytosis oxidase/Bem1p domain-containing proteinPB1CP negatively regulates the NADPH oxidase RBOHD inplant immunity. New

Phytologist, 2023 accepted.
Google Scholar: Author Only Title Only Author and Title

Grison, M.S., Kirk, P., Brault, M.L., Wu, X.N., Schulze, W.X., Benitez-Alfonso, Y., Immel, F., and Bayer, E.M. (2019). Plasma Membrane-Associated Receptor-like Kinases Relocalize to Plasmodesmata in Response to Osmotic Stress. Plant Physiol 181, 142-160.
Google Scholar: Author Only Title Only Author and Title

Gully, K., Pelletier, S., Guillou, M.C., Ferrand, M., Aligon, S., Pokotylo, I., Perrin, A., Vergne, E., Fagard, M., Ruelland, E., Grappin, P., Bucher, E., Renou, J.P., and Aubourg, S. (2019). The SCOOP12 peptide regulates defense response and root elongation in Arabidopsis thaliana. J Exp Bot 70, 1349-1365.
Google Scholar: Author Only Title Only Author and Title

Guzman, A.R., Kim, J.G., Taylor, K.W., Lanver, D., and Mudgett, M.B. (2020). Tomato Atypical Receptor Kinase1 Is Involved in the Regulation of Preinvasion Defense. Plant Physiol 183, 1306-1318.
Google Scholar: Author Only Title Only Author and Title

Heese, A., Hann, D.R., Gimenez-Ibanez, S., Jones, A.M., He, K., Li, J., Schroeder, J.I., Peck, S.C., and Rathjen, J.P. (2007). The receptor-like kinase SERK3/BAK1 is a central regulator of innate immunity in plants. Proc Natl Acad Sci U S A 104, 12217-12222.
Google Scholar: Author Only Title Only Author and Title

Hou, S., Liu, D., Huang, S., Luo, D., Liu, Z., Xiang, Q., Wang, P., Mu, R., Han, Z., Chen, S., Chai, J., Shan, L., and He, P. (2021). The Arabidopsis MIK2 receptor elicits immunity by sensing a conserved signature from phytocytokines and microbes. Nat Commun 12, 5494.
Google Scholar: Author Only Title Only Author and Title

Hurley, B., Lee, D., Mott, A., Wilton, M., Liu, J., Liu, Y.C., Angers, S., Coaker, G., Guttman, D.S., and Desveaux, D. (2014). The Pseudomonas syringae type III effector HopF2 suppresses Arabidopsis stomatal immunity. PLoS One 9, e114921.
Google Scholar: Author Only Title Only Author and Title

Ishiwata-Endo, H., Kato, J., Stevens, L.A., and Moss, J. (2020). ARH1 in Health and Disease. Cancers (Basel) 12.
Google Scholar: Author Only Title Only Author and Title

Isner, J.C., Begum, A., Nuehse, T., Hetherington, A.M., and Maathuis, F.J.M. (2018). KIN7 Kinase Regulates the Vacuolar TPK1 K(+) Channel during Stomatal Closure. Curr Biol 28, 466-472 e464.
Google Scholar: Author Only Title Only Author and Title

Kadota, Y., Shirasu, K., and Zipfel, C. (2015). Regulation of the NADPH Oxidase RBOHD During Plant Immunity. Plant Cell Physiol 56, 1472-1480.
Google Scholar: Author Only Title Only Author and Title

Kadota, Y., Sklenar, J., Derbyshire, P., Stransfeld, L., Asai, S., Ntoukakis, V., Jones, J.D., Shirasu, K., Menke, F., Jones, A., and Zipfel, C. (2014). Direct regulation of the NADPH oxidase RBOHD by the PRR-associated kinase BIK1 during plant immunity. Mol Cell 54, 43-55.
Google Scholar: Author Only Title Only Author and Title

Keinath, N.F., Kierszniowska, S., Lorek, J., Bourdais, G., Kessler, S.A., Shimosato-Asano, H., Grossniklaus, U., Schulze, W.X., Robatzek, S., and Panstruga, R. (2010). PAMP (Pathogen-associated Molecular Pattern)-induced Changes in Plasma Membrane Compartmentalization Reveal Novel Components of Plant Immunity. Journal of Biological Chemistry 285, 39140-39149.
Google Scholar: Author Only Title Only Author and Title

Khan, M., Youn, J.Y., Gingras, A.C., Subramaniam, R., and Desveaux, D. (2018). In planta proximity dependent biotin identification (BioID). Sci Rep 8, 9212.
Google Scholar: Author Only Title Only Author and Title

Kim, J.G., Li, X., Roden, J.A., Taylor, K.W., Aakre, C.D., Su, B., Lalonde, S., Kirik, A., Chen, Y., Baranage, G., McLane, H., Martin, G.B., and Mudgett, M.B. (2009). Xanthomonas T3S Effector XopN Suppresses PAMP-Triggered Immunity and Interacts with a Tomato Atypical Receptor-Like Kinase and TFT1. Plant Cell 21, 1305-1323.
Google Scholar: Author Only Title Only Author and Title

Kutschera, A., Dawid, C., Gisch, N., Schmid, C., Raasch, L., Gerster, T., Schaffer, M., Smakowska-Luzan, E., Belkhadir, Y., Vlot, A.C., Chandler, C.E., Schellenberger, R., Schwudke, D., Ernst, R.K., Dorey, S., Huckelhoven, R., Hofmann, T., and Ranf, S. (2019). Bacterial medium-chain 3-hydroxy fatty acid metabolites trigger immunity in Arabidopsis plants. Science 364, 178-181.
Google Scholar: Author Only Title Only Author and Title

Lewis, J.D., Abada, W., Ma, W., Guttman, D.S., and Desveaux, D. (2008). The HopZ family of Pseudomonas syringae type III effectors require myristoylation for virulence and avirulence functions in Arabidopsis thaliana. J Bacteriol 190, 2880-2891.
Google Scholar: Author Only Title Only Author and Title

Lewis, J.D., Wan, J., Ford, R., Gong, Y., Fung, P., Nahal, H., Wang, P.W., Desveaux, D., and Guttman, D.S. (2012). Quantitative

Interactor Screening with next-generation Sequencing (QIS-Seq) identifies Arabidopsis thaliana MLO2 as a target of the Pseudomonas syringae type III effector HopZ2. BMC Genomics 13, 8.
Google Scholar: Author Only Title Only Author and Title

Li, L., Kim, P., Yu, L., Cai, G., Chen, S., Alfano, J.R., and Zhou, J.M. (2016). Activation-Dependent Destruction of a Co-receptor by a Pseudomonas syringae Effector Dampens Plant Immunity. Cell Host Microbe 20, 504-514.
Google Scholar: Author Only Title Only Author and Title

Li, L., Li, M., Yu, L.P., Zhou, Z.Y., Liang, X.X., Liu, Z.X., Cai, G.H., Gao, L.Y., Zhang, X.J., Wang, Y.C., Chen, S., and Zhou, J.M. (2014). The FLS2-Associated Kinase BIK1 Directly Phosphorylates the NADPH Oxidase RbohD to Control Plant Immunity. Cell Host & Microbe 15, 329-338.
Google Scholar: Author Only Title Only Author and Title

Liang, X.X., Ding, P.T., Liang, K.H., Wang, J.L., Ma, M.M., Li, L., Li, L., Li, M., Zhang, X.J., Chen, S., Zhang, Y.L., and Zhou, J.M. (2016). Arabidopsis heterotrimeric G proteins regulate immunity by directly coupling to the FLS2 receptor. Elife 5, e13568.
Google Scholar: Author Only Title Only Author and Title

Liu, Z.X., Wu, Y., Yang, F., Zhang, Y.Y., Chen, S., Xie, Q., Tian, X.J., and Zhou, J.M. (2013). BIK1 interacts with PEPRs to mediate ethylene-induced immunity. P Natl Acad Sci USA 110, 6205-6210.
Google Scholar: Author Only Title Only Author and Title

Lu, D.P., Wu, S.J., Gao, X.Q., Zhang, Y.L., Shan, L.B., and He, P. (2010). A receptor-like cytoplasmic kinase, BIK1, associates with a flagellin receptor complex to initiate plant innate immunity. P Natl Acad Sci USA 107, 496-501.
Google Scholar: Author Only Title Only Author and Title

Ma, M.M., Wang, W., Fei, Y., Cheng, H.Y., Song, B.B., Zhou, Z.Y., Zhao, Y., Zhang, X.J., Li, L., Chen, S., Wang, J.Z., Liang, X.X., and Zhou, J.M. (2022). A surface-receptor-coupled G protein regulates plant immunity through nuclear protein kinases. Cell Host & Microbe 30, 1602-+.
Google Scholar: Author Only Title Only Author and Title

Macho, A.P., and Zipfel, C. (2014). Plant PRRs and the activation of innate immune signaling. Mol Cell 54, 263-272.
Google Scholar: Author Only Title Only Author and Title

Mbengue, M., Bourdais, G., Gervasi, F., Beck, M., Zhou, J., Spallek, T., Bartels, S., Boller, T., Ueda, T., Kuhn, H., and Robatzek, S. (2016). Clathrin-dependent endocytosis is required for immunity mediated by pattern recognition receptor kinases. Proc Natl Acad Sci U S A 113, 11034-11039.
Google Scholar: Author Only Title Only Author and Title

Melotto, M., Underwood, W., Koczan, J., Nomura, K., and He, S.Y. (2006). Plant stomata function in innate immunity against bacterial invasion. Cell 126, 969-980.
Google Scholar: Author Only Title Only Author and Title

Miller, J.C., Lawrence, S.A., and Clay, N.K. (2019). Heterotrimeric G proteins promote FLS2 protein accumulation through inhibition of FLS2 autophagic degradation. bioRxiv, 438135.
Google Scholar: Author Only Title Only Author and Title

Nekrasov, V., Li, J., Batoux, M., Roux, M., Chu, Z.H., Lacombe, S., Rougon, A., Bittel, P., Kiss-Papp, M., Chinchilla, D., van Esse, H.P., Jorda, L., Schwessinger, B., Nicaise, V., Thomma, B.P., Molina, A., Jones, J.D., and Zipfel, C. (2009). Control of the pattern-recognition receptor EFR by an ER protein complex in plant immunity. EMBO J 28, 3428-3438.
Google Scholar: Author Only Title Only Author and Title

Nicaise, V., Joe, A., Jeong, B.R., Korneli, C., Boutrot, F., Westedt, I., Staiger, D., Alfano, J.R., and Zipfel, C. (2013). Pseudomonas HopU1 modulates plant immune receptor levels by blocking the interaction of their mRNAs with GRP7. EMBO J 32, 701-712.
Google Scholar: Author Only Title Only Author and Title

Rhodes, J., Yang, H., Moussu, S., Boutrot, F., Santiago, J., and Zipfel, C. (2021). Perception of a divergent family of phytocytokines by the Arabidopsis receptor kinase MIK2. Nat Commun 12, 705.
Google Scholar: Author Only Title Only Author and Title

Robatzek, S., Chinchilla, D., and Boller, T. (2006). Ligand-induced endocytosis of the pattern recognition receptor FLS2 in Arabidopsis. Genes Dev 20, 537-542.
Google Scholar: Author Only Title Only Author and Title

Roux, M., Schwessinger, B., Albrecht, C., Chinchilla, D., Jones, A., Holton, N., Malinovsky, F.G., Tor, M., de Vries, S., and Zipfel, C. (2011). The Arabidopsis leucine-rich repeat receptor-like kinases BAK1/SERK3 and BKK1/SERK4 are required for innate immunity to hemibiotrophic and biotrophic pathogens. Plant Cell 23, 2440-2455.
Google Scholar: Author Only Title Only Author and Title

Scheuring, D., Viotti, C., Kruger, F., Kunzl, F., Sturm, S., Bubeck, J., Hillmer, S., Frigerio, L., Robinson, D.G., Pimpl, P., and Schumacher, K. (2011). Multivesicular bodies mature from the trans-Golgi network/early endosome in Arabidopsis. Plant Cell 23,

3463-3481.
Google Scholar: Author Only Title Only Author and Title

Smakowska-Luzan, E., Mott, G.A., Parys, K., Stegmann, M., Howton, T.C., Layeghifard, M., Neuhold, J., Lehner, A., Kong, J., Grunwald, K., Weinberger, N., Satbhai, S.B., Mayer, D., Busch, W., Madalinski, M., Stolt-Bergner, P., Provart, N.J., Mukhtar, M.S., Zipfel, C., Desveaux, D., Guttman, D.S., and Belkhadir, Y. (2018). An extracellular network of Arabidopsis leucine-rich repeat receptor kinases. Nature 553, 342-346.
Google Scholar: Author Only Title Only Author and Title

Stegmann, M., Zecua-Ramirez, P., Ludwig, C., Lee, H.S., Peterson, B., Nimchuk, Z.L., Belkhadir, Y., and Huckelhoven, R. (2022). RGI-GOLVEN signaling promotes cell surface immune receptor abundance to regulate plant immunity. EMBO Rep 23, e53281.
Google Scholar: Author Only Title Only Author and Title

Taylor, K.W., Kim, J.G., Su, X.B., Aakre, C.D., Roden, J.A., Adams, C.M., and Mudgett, M.B. (2012). Tomato TFT1 is required for PAMP-triggered immunity and mutations that prevent T3S effector XopN from binding to TFT1 attenuate Xanthomonas virulence. PLoS Pathog 8, e1002768.
Google Scholar: Author Only Title Only Author and Title

Thor, K., Jiang, S., Michard, E., George, J., Scherzer, S., Huang, S., Dindas, J., Derbyshire, P., Leitao, N., DeFalco, T.A., Koster, P., Hunter, K., Kimura, S., Gronnier, J., Stransfeld, L., Kadota, Y., Bucherl, C.A., Charpentier, M., Wrzaczek, M., MacLean, D., Oldroyd, G.E.D., Menke, F.L.H., Roelfsema, M.R.G., Hedrich, R., Feijo, J., and Zipfel, C. (2020). The calcium-permeable channel OSCA1.3 regulates plant stomatal immunity. Nature 585, 569-573.
Google Scholar: Author Only Title Only Author and Title

Tian, W., Hou, C.C., Ren, Z.J., Wang, C., Zhao, F.G., Dahlbeck, D., Hu, S.P., Zhang, L.Y., Niu, Q., Li, L.G., Staskawicz, B.J., and Luan, S. (2019). A calmodulin-gated calcium channel links pathogen patterns to plant immunity. Nature 572, 131-+.
Google Scholar: Author Only Title Only Author and Title

Wang, J., Xi, L., Wu, X.N., Konig, S., Rohr, L., Neumann, T., Weber, J., Harter, K., and Schulze, W.X. (2022). PEP7 acts as a peptide ligand for the receptor kinase SIRK1 to regulate aquaporin-mediated water influx and lateral root growth. Mol Plant 15, 1615-1631.
Google Scholar: Author Only Title Only Author and Title

Wang, Y., Li, J., Hou, S., Wang, X., Li, Y., Ren, D., Chen, S., Tang, X., and Zhou, J.M. (2010). A Pseudomonas syringae ADP-ribosyltransferase inhibits Arabidopsis mitogen-activated protein kinase kinases. Plant Cell 22, 2033-2044.
Google Scholar: Author Only Title Only Author and Title

Wilton, M., Subramaniam, R., Elmore, J., Felsensteiner, C., Coaker, G., and Desveaux, D. (2010). The type III effector HopF2 Pto targets Arabidopsis RIN4 protein to promote Pseudomonas syringae virulence. Proceedings of the National Academy of Sciences 107, 2349-2354.
Google Scholar: Author Only Title Only Author and Title

Wu, S., Lu, D., Kabbage, M., Wei, H.L., Swingle, B., Records, A.R., Dickman, M., He, P., and Shan, L. (2011). Bacterial effector HopF2 suppresses arabidopsis innate immunity at the plasma membrane. Mol Plant Microbe Interact 24, 585-593.
Google Scholar: Author Only Title Only Author and Title

Wu, X.N., Chu, L., Xi, L., Pertl-Obermeyer, H., Li, Z., Sklodowski, K., Sanchez-Rodriguez, C., Obermeyer, G., and Schulze, W.X. (2019). Sucrose-induced Receptor Kinase 1 is Modulated by an Interacting Kinase with Short Extracellular Domain. Mol Cell Proteomics 18, 1556-1571.
Google Scholar: Author Only Title Only Author and Title

Xiang, T.T., Zong, N., Zou, Y., Wu, Y., Zhang, J., Xing, W.M., Li, Y., Tang, X.Y., Zhu, L.H., Chai, J.J., and Zhou, J.M. (2008). Pseudomonas syringae effector AvrPto blocks innate immunity by targeting receptor kinases. Current Biology 18, 74-80.
Google Scholar: Author Only Title Only Author and Title

Xu, J., Xie, J., Yan, C.F., Zou, X.Q., Ren, D.T., and Zhang, S.Q. (2014). A chemical genetic approach demonstrates that MPK3/MPK6 activation and NADPH oxidase-mediated oxidative burst are two independent signaling events in plant immunity. Plant Journal 77, 222-234.
Google Scholar: Author Only Title Only Author and Title

Yang, F., Kimberlin, A.N., Elowsky, C.G., Liu, Y., Gonzalez-Solis, A., Cahoon, E.B., and Alfano, J.R. (2019). A Plant Immune Receptor Degraded by Selective Autophagy. Mol Plant 12, 113-123.
Google Scholar: Author Only Title Only Author and Title

Yeh, Y.H., Panzeri, D., Kadota, Y., Huang, Y.C., Huang, P.Y., Tao, C.N., Roux, M., Chien, H.C., Chin, T.C., Chu, P.W., Zipfel, C., and Zimmerli, L. (2016). The Arabidopsis Malectin-Like/LRR-RLK IOS1 Is Critical for BAK1-Dependent and BAK1-Independent Pattern-Triggered Immunity. Plant Cell 28, 1701-1721.
Google Scholar: Author Only Title Only Author and Title

Zhang, J., Li, W., Xiang, T.T., Liu, Z.X., Laluk, K., Ding, X.J., Zou, Y., Gao, M.H., Zhang, X.J., Chen, S., Mengiste, T., Zhang, Y.L., and Zhou, J.M. (2010). Receptor-like Cytoplasmic Kinases Integrate Signaling from Multiple Plant Immune Receptors and Are

Targeted by a Pseudomonas syringae Effector. Cell Host & Microbe 7, 290-301.
Google Scholar: Author Only Title Only Author and Title

Zhou, J., Wu, S., Chen, X., Liu, C., Sheen, J., Shan, L., and He, P. (2014). The Pseudomonas syringae effector HopF2 suppresses Arabidopsis immunity by targeting BAK1. Plant J 77, 235-245.
Google Scholar: Author Only Title Only Author and Title

Supporting Information